



HAL
open science

Quantifying the dominant sources of sediment in a drained lowland agricultural catchment: The application of a thorium-based particle size correction in sediment fingerprinting

Anthony Foucher, Patrick J. Lacey, Sébastien Salvador-Blanes, O. Evrard, Marion Le Gall, Irène Lefèvre, Olivier Cerdan, Vignesh Rajkumar, Marc Desmet

► To cite this version:

Anthony Foucher, Patrick J. Lacey, Sébastien Salvador-Blanes, O. Evrard, Marion Le Gall, et al.. Quantifying the dominant sources of sediment in a drained lowland agricultural catchment: The application of a thorium-based particle size correction in sediment fingerprinting. *Geomorphology*, 2015, 250, pp.271 - 281. 10.1016/j.geomorph.2015.09.007 . hal-01400992

HAL Id: hal-01400992

<https://brgm.hal.science/hal-01400992>

Submitted on 26 May 2020

HAL is a multi-disciplinary open access archive for the deposit and dissemination of scientific research documents, whether they are published or not. The documents may come from teaching and research institutions in France or abroad, or from public or private research centers.

L'archive ouverte pluridisciplinaire **HAL**, est destinée au dépôt et à la diffusion de documents scientifiques de niveau recherche, publiés ou non, émanant des établissements d'enseignement et de recherche français ou étrangers, des laboratoires publics ou privés.

1 —Quantifying the dominant sources of sediment in a drained lowland agricultural catchment: the
2 application of a thorium-based particle size correction in sediment fingerprinting

3
4
5 Anthony Foucher ^{a,*}, J. Patrick Lacey ^b, Sébastien Salvador-Blanes ^a, Olivier Evrard ^b, Marion Le
6 Gall ^b, Irène Lefèvre ^b, Olivier Cerdan ^c, Vignesh Rajkumar ^{a,d}, Marc Desmet ^a

7
8
9 ^aE.A. 6293 GéHCO, GéoHydrosystèmes COntinentaux, Université F. Rabelais de Tours, Faculté des Sciences et
10 Techniques, Parc de Grandmont, 37200 Tours, France

11 ^bLaboratoire des Sciences du Climat et de l'Environnement (LSCE/IPSL), UMR 8212 (CEA-CNRS-UVSQ),
12 Avenue de la Terrasse, 91198 Gif-sur-Yvette Cedex, France

13 ^cDépartement Risques et Prévention, Bureau de Recherches Géologiques et Minières, 3 avenue Claude
14 Guillemin, 45060 Orléans, France

15 ^dCentre for Water Resources, CEG, Anna University, Sardar Patel Rd, Chennai, Tamil Nadu 600025, India

16
17
18 * **Corresponding author:** Anthony.foucher@univ-tours.fr; Tel: (33) 247367090

34 **Abstract**

35

36 Soil erosion is one of the main factors influencing land degradation and water quality at the global
37 scale. Identifying the main sediment sources is therefore essential for the implementation of
38 appropriate soil erosion mitigation measures. Accordingly, caesium-137 (^{137}Cs) concentrations were
39 used to determine the relative contribution of surface and subsurface erosion sources in a lowland
40 drained catchment in France. As ^{137}Cs concentrations are often dependent on particle size, specific
41 surface area (*SSA*) and novel Thorium (*Th*) based particle size corrections were applied. Surface and
42 subsurface samples were collected to characterize the radionuclide properties of potential sources.
43 Sediment samples were collected during one hydrological year and a sediment core was sampled to
44 represent sediment accumulated over a longer temporal period. Additionally, sediment from tile drains
45 was sampled to determine the radionuclide properties of sediment exported from the drainage network.
46 A distribution modeling approach was used to quantify the relative sediment contributions from
47 surface and subsurface sources. The results highlight a substantial enrichment in fine particles and
48 associated ^{137}Cs concentrations between the sources and the sediment. The application of both
49 correction factors reduced this difference, with the *Th* correction providing a more accurate
50 comparison of source and sediment samples than the *SSA* correction. Modelling results clearly indicate
51 the dominance of surface sources during the flood events and in the sediment core. Sediment exported
52 from the drainage network was modelled to originate predominantly from surface sources. This study
53 demonstrates the potential of *Th* to correct for ^{137}Cs particle size enrichment. More importantly, this
54 research indicates that drainage networks may significantly increase the connectivity of surface
55 sources to stream networks. Managing sediment transferred through drainage networks may reduce the
56 deleterious effects of suspended sediment loads on riverine systems in similar lowland drained
57 agricultural catchments.

58

59 **Key Words:** Sediment tracing, Agricultural lowland areas, Cesium-137, Particle size correction, Tile
60 drainage networks

61

62 **Highlights:**

- 63 • Source and sediment caesium-137 activities were used to trace sediment sources
- 64 • Two particle size corrections were compared to address enrichment in fine particles
- 65 • A thorium-based correction out performed a specific surface area correction
- 66 • Sediment in this lowland agricultural catchment is supplied by surface sources
- 67 • Drainage networks may increase the connectivity of surface sources to rivers

68

69

70

71

72 1. Introduction

73

74 Soil erosion by water affects a significant proportion (16%) of agricultural land in Europe
75 (Cerdan et al., 2010; Jones et al., 2012). Although natural, this degradation process is accelerated by
76 land use change and anthropogenic pressures in agricultural landscapes (Bakker et al., 2008; Chartin et
77 al., 2011; Sharma et al., 2011). Around the world, the negative effects of soil erosion are characterized
78 by the decline of crop yields, the reduction of soil water storage capacity and decreases in soil organic
79 matter (Berger et al., 2006; Boardman and Poesen, 2006). The main problems associated with
80 accelerated soil erosion are often not only the actual soil loss itself, rather the adverse effects of
81 elevated suspended sediment yields and adsorbed contaminants downstream (Walling et al., 2003).

82 The excess of fine sediment particles (e.g., $<63 \mu\text{m}$) associated with soil erosion are
83 detrimental to water quality and stream environments (Kronvang et al., 2003; Owens et al., 2005;
84 Horowitz, 2008). Elevated fine sediment loads can result in numerous problems such as elevated
85 turbidity and reservoir siltation (Wood and Armitage, 1997; Nakamura et al., 2004). Importantly, fine
86 sediments often transport contaminants such as heavy metals, Polychlorinated Biphenyls (PCB),
87 phosphorus, pesticides, pathogens, and fallout radionuclides (Desmet et al., 2012; Ayrault et al., 2014;
88 Evrard et al., 2014).

89 Currently, there is a limited understanding regarding the dominant sediment source in France
90 in particular, and in drained lowland cultivated areas in general (Russell et al., 2001; Walling et al.,
91 2002). The implementation of highly productive cropland agriculture practices in these regions has
92 included the installation of drainage networks that induce a high level of connectivity between eroding
93 soils and river systems. Although these land management changes were clearly associated with
94 increased sediment yields (e.g Foster and Walling, 1994; Dearing and Jones, 2003; Ahn et al., 2008),
95 the identification of the dominant sediment sources, their dynamics, and their pathways in drained
96 landscapes with similar intensive agricultural practices remains poorly understood. Indeed, research
97 has highlighted the limited information available regarding sediment exported through drainage
98 networks in these environments (Kronvang et al., 1997; Walling and Collins, 2005; King et al., 2014).

99 To implement appropriate measures to reduce erosion and sediment production (Evrard et al.,
100 2008), it is essential to identify the dominant sediment sources and understand their dynamics.
101 Sediment fingerprinting techniques provide a direct method to identify and quantify sediment
102 contributions from different sources (Collins and Walling, 2002). The technique is based on the direct
103 comparison of sediment and source properties (Walling et al., 1993; Collins et al., 2010). A variety of
104 parameters have been used in sediment fingerprinting studies to discriminate between potential
105 sources, including geochemical composition, sediment color, plant pollen, and fallout radionuclides
106 (Brown, 1985; Walling et al., 2002; Martinez-Carreras et al., 2010). In particular, caesium-137 (^{137}Cs)

107 discriminates between surface and subsurface soils, regardless of other soil properties including
108 catchment geology (Wallbrink et al., 1996; Walling, 2005; Caitcheon et al., 2012).

109 ^{137}Cs ($t_{1/2} = 30$ years) is an artificial radionuclide originating from two main sources in
110 Western Europe: thermonuclear weapons testing (1950–1970s) and the Chernobyl accident. Fallout
111 from the Fukushima accident in 2011 was shown to be negligible in this region (Evrard et al., 2012).
112 ^{137}Cs is quickly and predominantly fixed to fine particles (He and Walling, 1996; Wallbrink and
113 Murray, 1996; Motha et al., 2002). In undisturbed soils, ^{137}Cs is concentrated near the soil surface (i.e.
114 within the top 10 cm), with concentrations decreasing exponentially with depth (Matisoff et al., 2002).
115 In cultivated soils, ^{137}Cs concentrations are homogenized by tillage (He and Walling, 1997; Matisoff et
116 al., 2002; Chartin et al., 2011). Accordingly, sediment generated from subsoil erosion processes, such
117 as channel bank erosion, will have low ^{137}Cs concentrations, whereas sediment generated from surface
118 soils will have elevated ^{137}Cs concentrations (e.g. Caitcheon et al., 2012; Olley et al., 2013). Through
119 comparing sediment and source ^{137}Cs concentrations, it is possible to determine whether sediment is
120 derived from surface or subsurface sources.

121 Soil erosion processes result in the preferential mobilization and transfer of fine sediment
122 particles (He and Walling, 1996). To reduce the impacts of grain size selectivity, many fingerprinting
123 studies isolate either the $<10\ \mu\text{m}$ (Olley and Caitcheon, 2000; Wallbrink, 2004) or the $<63\ \mu\text{m}$ fraction
124 (Navratil et al., 2012; Pulley et al., 2015) to mitigate differences in the particle size distributions of
125 source soil and sediment. To further reduce the grain size effect when tracing sediment, a correcting
126 factor has been applied (Collins et al., 1996). This correction is based on the specific surface area
127 (SSA) of sediment and source soils, and it relies on the assumption of positive linearity between SSA
128 and tracer property concentrations. Linear particle size correction factors may be useful when there is
129 a narrow range of particle size differences between source soils and sediment (Koiter et al., 2013).
130 This particle size correction has been applied to various tracers, such as radionuclides (He and Owens,
131 1995; He and Walling, 1996), phosphorus (Owens and Walling, 2002) and extractable metals
132 (Horowitz and Elrick, 1987).

133 Although this particle size correction has been widely applied (Collins et al., 2001; Carter et
134 al., 2003), there are acknowledged limitations (Koiter et al., 2013). For example, Smith and Blake
135 (2014) demonstrated that the most critical assumption, which could have large effects on source
136 apportionments, is the hypothesis of positive linearity between particle size and tracer concentration.
137 Contrary to previous studies, Smith and Blake (2014) demonstrated that this relationship does not
138 apply to all tracer properties and that the assumption of linearity must be routinely tested. Russell et al.
139 (2001) also demonstrated that the linear particle size correction relationship was inappropriate when
140 there were large SSA differences between sources.

141 Given the potential uncertainty associated with the SSA correction, some authors, such as
142 Martinez-Carreras et al. (2010), do not apply it. As an alternative to the SSA-derived correction,
143 Sakaguchi et al. (2006) demonstrated the potential of a Thorium (*Th*) normalization to correct for the

144 grain size effect in lake sediment cores. Owing to its measurement in gamma spectrometry along with
145 ^{137}Cs , there is a novel utility in the potential for *Th* to correct for grain size differences that could
146 remove the need for simultaneous *SSA* measurements in sediment fingerprinting studies using fallout
147 radionuclides for source discrimination.

148 The objective of this research is to identify the dominant sediment sources and their temporal
149 variation in the Louroux catchment, France; a small agricultural catchment, representative of the
150 lowland drained landscapes of Western Europe. To determine the main source of sediment in the
151 Louroux catchment, first we examine particle size effects and compare the impacts of *Th* and *SSA*
152 corrections on ^{137}Cs soil and channel bank concentrations. Second, we characterize the ^{137}Cs
153 concentrations of surface and subsurface sources. Third, we model the relative contribution of these
154 sources to sediment sampled throughout a year, a sediment core collected in a pond at the outlet of the
155 catchment, and sediment sampled within the tile drainage network.

156

157 2. Materials and methods

158

159 2.1. Study area

160

161 The Louroux pond catchment (24 km²) is a headwater agricultural basin located in the central
162 part of the Loire River basin, France (Fig. 1). The catchment is characterized by a flat topography
163 (average slope 0.44%; altitude ranging from 94 to 129 m). The catchment surface is primarily
164 occupied by arable land (78%), followed by pasture (18%) and forest (4%) (European Environment
165 Agency, 2002). The climate is temperate oceanic with a mean annual rainfall of 684 mm (between
166 1971–2000). The bedrock consists of carbonates, detrital and loess deposits (Rasplus et al., 1982).
167 Soils are classified as Epistagnic Luvic Cambisols, which are predominantly hydromorphic and prone
168 to surface crusting (Froger et al., 1994).

169 This basin, like the majority of the great western agricultural plain in Europe, has undergone a
170 global modernization of agricultural practices and land use changes. Two land consolidation schemes
171 were implemented in the catchment in 1954 and 1992. Stream networks were created or redesigned,
172 and tile drainage networks were installed to drain the hydromorphic soils.

173 The Louroux pond, located at the catchment outlet (52 ha; Fig. 1), was created during the
174 Middle-Ages (1000 AD). Recent research indicated that a significant increase in soil erosion in the
175 catchment during the last 70 years resulted in the accelerated sedimentation and eutrophication of the
176 pond (Foucher et al., 2015). Over the last decade, the Louroux pond has received an annual average
177 input of 2500 tons of terrigenous material (Foucher et al., 2015).

178

179 2.2 Sampling

180

181 2.2.1. Soil and stream bank sampling

182 Soil samples from ground surfaces and subsurface material exposed on actively eroding river
183 banks were collected from January 2013 to February 2014. Sampling was restricted to cropland areas,
184 as soil erosion was shown to be negligible under grassland in similar environments of Northwestern
185 Europe (Cerdan et al., 2002; Evrard et al., 2010). In addition, grassland areas in this catchment are
186 ploughed approximately every 10 years, mixing ^{137}Cs in the soil profile similarly to croplands.

187 Surface sources ($n = 34$) were sampled by scraping the top 2–3 cm layer of soil with a plastic
188 spatula in potentially eroding areas directly connected to the stream network. Each of these surface
189 source composite samples was comprised of five sub-samples collected within an area of 5 m².
190 Subsurface sources ($n = 15$) were sampled by scraping a 2–3 cm layer of the actively eroding bank
191 face. In addition, sediment was collected in hillslopes during the rain by placing plastic bottles on the
192 hillslope surface to sample sediment during runoff events ($n = 3$). These plastic bottles were collected
193 after events along with the deposited sediment.

194

195 2.2.2. Suspended sediment sampling

196 Hydro-sedimentary parameters were continuously recorded at five automated monitoring sites
197 (S1–S5, Fig. 1). Water discharge was measured using a v-notch weir. Suspended sediment was
198 continuously measured using a Ponsel[®] calibrated turbidity sensor. Twenty-four liters of river water
199 were automatically collected according to the water level at each station during five flood events ($n =$
200 21) and once during the low-water period ($n = 4$) to examine variability throughout the hydrological
201 year in 2013–2014. All individual samples for each station and for each flood were mixed to prepare
202 composite samples. In addition to the river monitoring sites, three stations were installed at tile drain
203 outlets to characterize the properties of the material transiting through the drainage networks and to
204 determine if sediment exported from this network had ^{137}Cs concentrations similar to surface or
205 subsurface sources (Fig. 1). To characterize the origin of sediment accumulated over a longer temporal
206 period (2003–2013) at the catchment outlet (Fig. 1), the top 10 cm of a 110 cm long core collected in
207 March 2013 was subsampled in 3 cm increments. This sediment core was sampled in the central pond
208 depression, an area that is representative of sediment deposition in the Louroux Pond. More details on
209 the core sampling and fallout radionuclide dating are provided in Foucher et al. (2015).

210

211 2.3. Sample treatment and analysis

212

213 Suspended sediment concentrations for the composite samples were determined by weighing
214 after filtration (40 microns acetate filters). Particle size analyses were performed on all suspended
215 sediment samples as well as on randomly selected source samples ($n = 18$) after removing carbonates

216 and organic material with hydrogen peroxide. Particle size was analysed with laser granulometry
217 (Malvern Mastersizer[®]) characterizing the textural parameters ranging between 0.01 and 3500 μm .

218 Randomly selected subsamples of subsurface ($n = 5$) and surface sources ($n = 5$) were sieved
219 to determine radionuclide activities in different particle size fractions. Samples were mechanically
220 sieved to 63 and 50 μm . The <20 μm fraction was then isolated by using the settling velocity
221 relationship predicted by Stokes' Law. These analyses were used to calculate the difference between
222 the bulk samples and the sieved samples, and to examine the utility of the two different corrections.

223 Suspended sediments collected during the flood events were flocculated using calcium
224 hydroxide (CaOH_2), to recover and concentrate radionuclides. For the measurement of radionuclides,
225 ~ 80 g of material was analysed for source samples and ~ 10 g for sediment samples. Activities were
226 determined by gamma spectrometry using low background coaxial N and P type GeHP detectors
227 (Canberra/Ortec) at the Laboratoire des Sciences du Climat et de l'Environnement (France) (Evrard et
228 al., 2011). Radionuclides activities were decay-corrected to the sampling date. In addition to the
229 radionuclide measurement, *Th* concentrations expressed in ppm were calculated from ^{228}Th activity
230 concentrations. Only ^{137}Cs is modelled in this study as only one tracer is required to discriminate
231 between two sources.

232

233 2.4. Particle size corrections

234

235 To limit the bias potentially introduced by particle size difference between sources and
236 sediment, a correcting factor used by Collins et al. (1996) was applied to radionuclide activities. This
237 approach is based on the ratio of *SSA* of each individual sediment sample to the mean *SSA* of each
238 source type, multiplied by the mean activity for each source:

239

$$240 \text{ SSA correcting factor}_i = \frac{(SSA_i)}{(SSA_y)} \times T_y \quad (1)$$

241

242 where SSA_i = specific surface area for each individual sample (i), SSA_y = specific surface area for each
243 source type (y), and T_y = mean tracer concentration for each source type (y).

244

245 The *Th* content correction was calculated based on the ratio of the radionuclide concentration
246 normalized with $\ln(\text{Th})$ of each individual sample, to the mean radionuclide concentration normalized
247 with $\ln(\text{Th})$ of each source type, multiplied by the mean radionuclide concentration of each source:

248

249 $\ln(Th)_{correcting\ factor}_i = \frac{T_i / \ln(Th)_i}{T_y / \ln(Th)_y} \times T_y$ (2)

250

251 where T_i = the tracer concentration for each individual sample (i), $\ln(Th)_i$ = the logarithm of the Th
 252 concentration (in ppm) for each individual sample (i), and $\ln(Th)_y$ = the logarithm of the Th
 253 concentration (in ppm) for each source type (y).

254 The SSA and Th corrections were applied for randomly selected soil ($n = 10$) and channel bank
 255 samples ($n = 7$) to test the relationship between the corrected and measured ^{137}Cs values. These results
 256 were then used to calculate the corrected values of ^{137}Cs with the SSA and Th correction factors of Eqs.
 257 (1) and (2). These corrected and measured values are first plotted to deduce equations from these
 258 relationships. These relations are then used to correct the entire dataset for each source type and for
 259 both correction techniques. To check the applicability of these corrections, sediment samples were
 260 collected on hillslopes during different hydrological periods and the ^{137}Cs activities measured for these
 261 samples were compared to these corrected values.

262

263

264 2.5. Distribution modelling

265

266 Distribution modelling approaches have been recently applied to sediment tracing research
 267 analyzing fallout radionuclides and elemental geochemistry (Caitcheon et al., 2012; Olley et al., 2013;
 268 Laceby and Olley, 2015). This modelling approach incorporates distributions throughout the entire
 269 modelling framework, including the relative contribution terms (i.e. not only source and in-stream
 270 components).

271 To determine the relative source contribution to in-stream sediment, it is assumed that the
 272 sediment samples are derived from a discrete mixture of sources with surface sources contributing x
 273 and subsurface sources contributing $1 - x$. With the distribution modelling approach, x is modelled as
 274 a truncated normal distribution ($0 \leq x \leq 1$), with a mixture mean (μ_m) and standard deviation (σ_m).
 275 Distributions of ^{137}Cs activities in surface (A) and subsurface (B) sources are then modelled when
 276 determining the relative source contributions (x) to in-stream sediment based on the following
 277 equation:

278

279 $Ax + B(1-x) = C$ (3)

280

281 where C is the in-stream sediment distribution. Normal distributions were modelled for source and
 282 sediment distributions as Laceby and Olley (2015) demonstrated that they resulted in more accurate
 283 modelling results compared to Student's t distributions. Sediment collected from the core sample from
 284 the Louroux Pond and sediment obtained from the tile drainage network were first individually

285 modelled. Second, distributions were modelled for sediment sample groups for different flood events
286 and also the different monitoring stations.

287 The model was optimized with the Optquest algorithm in Oracle's Crystal Ball software. For
288 more details on the modelling approach, see Laceby and Olley (2015). In general, the optimal value of
289 x was determined by simultaneously solving Eq. (3) 2500 times with the Optquest algorithm. During
290 this simulation, 2500 Latin hypercube samples were drawn from the source (A and B) and in-stream
291 sediment (C) distributions while solving Eq. (3) by varying x , μ_m and σ_m . This simulation was then
292 repeated an additional 2500 times with the median of x for these additional simulations being reported
293 as the surface source proportional contribution to sampled sediment.

294 The model uncertainty for each sources' proportional contribution is calculated by summing
295 the modelled σ_m , with the median absolute deviation (MAD) of σ_m , and also the MAD of the modelled
296 source proportional contributions. The latter two components of model error are calculated from the
297 additional 2500 simulations. This model uncertainty combines actual σ_m for each source contribution
298 with the MAD of this standard deviation and the MAD of the actual source contribution (x) for the
299 additional 2500 simulations.

300

301

302 3. Results

303

304 3.1. Correction of grain size effects

305

306 Particle size analyses highlight differences between the D_{50} (median particle size) of the
307 surface ($32.2 \pm 7 \mu\text{m}$) and subsurface sources ($38.5 \pm 8 \mu\text{m}$) in comparison to the in-stream sediment
308 ($6.2 \pm 2 \mu\text{m}$). A t -test between the two sources did not show a significant difference between their D_{50}
309 (p -value = 0.14). Significant differences were found between D_{50} of surface sources and in-stream
310 sediment ($p = 0.00$) and also between subsurface sources and in-stream sediment samples ($p = 0.00$).
311 In addition, soil samples collected before and during runoff events clearly highlight the particle size
312 enrichment during sediment generation processes, with an average activity measured before the runoff
313 of $3.7 \pm 3 \text{ Bq kg}^{-1}$ compared to $17 \pm 3 \text{ Bq kg}^{-1}$ during runoff. These samples demonstrate a difference
314 of 78% between surface sources and generated sediment, with an enrichment factor of 4.6.

315 The significant particle size effect noted above may prevent the direct comparison between
316 bulk sources and sediment samples. To test the impact of this effect on radionuclide activities, several
317 source samples were fractionated. The results from five soil samples highlight an enrichment factor of
318 2 between the bulk and the $<20 \mu\text{m}$ particle size fraction for the soil samples and the absence of
319 detectable ^{137}Cs in the 20-50 μm fraction for these samples (Fig. 2). There is an 80% difference
320 between the bulk and sediment particle size which can impact modelling results. For the 63 μm

321 fraction, this difference is reduced to 77% compared to 64% for the 20 μm fraction. Isolating the <20
322 μm fraction does not allow for a direct comparison between the sources and the suspended sediment.
323 The particle size enrichment of ^{137}Cs concentrations is plotted in Fig. 3 demonstrating clearly that
324 sediment samples collected during the flood events are distinct from the source soils. To address this
325 particle size effect and allow for comparison between sources and sediment samples, source activities
326 were corrected with two distinct particle size proxies.

327 *SSA*, *Th* and ^{137}Cs activities measured for soil ($n = 10$) and channel bank samples ($n = 7$) were
328 plotted to deduce the relationships between the corrected and measured values (Fig. 4). These plots
329 demonstrate that for the *SSA* correction a strong linear relationship exists between the corrected values
330 and measured ^{137}Cs activities in the soil ($r^2 = 0.89$) and channel bank samples ($r^2 = 0.94$) (Fig. 4). The
331 *Th* particle size correction, based on $\ln(\text{Th})$ normalization, also had a strong exponential relationship
332 for the channel bank samples ($r^2 = 0.98$) and surface soil samples ($r^2 = 0.96$). Both corrections have a
333 similar relationship for the subsurface samples. In contrast, the relationship obtained for the surface
334 samples was different. The ^{137}Cs activities after the *SSA* correction ranged between 3.2 and 20 Bq kg^{-1}
335 whereas the ^{137}Cs activities after the *Th* normalization ranged between 1 and 30 Bq kg^{-1} . For both
336 approaches, the mean values are comparable, 9.3 and 10.2 Bq kg^{-1} for the *SSA* and *Th* corrections
337 respectively. The difference was the wider range with the *Th* correction.

338 As particle size data were available for only part of the dataset, both correcting factors were
339 applied to the whole data set (subsurface sources $n = 15$ and surface sources $n = 34$) by using the
340 equations for the surface and subsurface samples shown in Fig. 4. The corrected data are plotted with
341 $^{210}\text{Pb}_{\text{ex}}$ in Fig. 5. After the application of both corrections, sediment ^{137}Cs activities generally plotted
342 within the ^{137}Cs activity range of the potential sources. With the *SSA* correction, five sediment samples
343 remain outside the source range (black squares in Fig. 5), whereas with the *Th* correction only one
344 sample plots outside the source range. Therefore, the *Th* correction likely provides a more direct
345 comparison with the sediment samples than the *SSA* correction.

346

347 3.2. ^{137}Cs concentration in source samples

348

349 Activities in the samples collected from stream banks range between 0 ± 0.3 and 3.1 ± 0.2 Bq
350 kg^{-1} with an average of 1.2 ± 0.2 Bq kg^{-1} . Soil surface activities range between 1 ± 0.1 and 7.9 ± 0.2
351 Bq kg^{-1} with an average of 3.2 ± 0.2 Bq kg^{-1} . These potential sources are statistically different ($p =$
352 0.00).

353 After the application of the *SSA* correction, the subsurface sample activities range between 0.7
354 and 5.1 Bq kg^{-1} (mean: 1.7 Bq kg^{-1}). These sample activities, after the *Th* correction, range between 0
355 and 6.5 Bq kg^{-1} (mean: 1.8 Bq kg^{-1}). The surface sample concentrations are more variable, ranging
356 between 3.7 and 23.8 Bq kg^{-1} (mean: 10 Bq kg^{-1}) after the *SSA* correction and between 0.8 and 35.5 Bq

357 kg^{-1} (mean: 11.2 Bq kg^{-1}) after the *Th* correction. Summary statistics of ^{137}Cs concentrations are
358 provided in Table 1.

359 The fitted normal distributions for surface and subsurface sources with both particle size
360 corrections are plotted in Fig. 6. The source samples are plotted in rank order. The source distribution
361 areas overlap only by 25% with the *SSA* correction compared to 62% with the *Th* correction. These
362 distributions are used to model the proportional contribution of the potential sources to suspended
363 sediment, the core samples, and the drainage network samples.

364

365 3.3. ^{137}Cs concentration in sediments samples

366

367 Activities of ^{137}Cs for the 23 sediment samples collected over the hydrological year range
368 between 6.1 ± 1 and $36.7 \pm 4.7 \text{ Bq kg}^{-1}$ with an average of $18.4 \pm 3.4 \text{ Bq kg}^{-1}$. The highest ^{137}Cs
369 activities have been recorded at the Masnier (station 3) and Grand Bray rivers (station 2) with average
370 ^{137}Cs activities of 19 ± 4.9 and $22.4 \pm 4.3 \text{ Bq kg}^{-1}$, respectively. For the other stations, ^{137}Cs activities
371 were similar (17.7 ± 3.6 , 16.7 ± 2 and $15.5 \pm 2.1 \text{ Bq kg}^{-1}$ for stations 1, 4 and 5). The flood event on
372 January 29, 2014 had the highest activity of all floods, with an average activity of $24.7 \pm 2.8 \text{ Bq kg}^{-1}$
373 followed by the flood of April 4, 2014 ($19.8 \pm 7.3 \text{ Bq kg}^{-1}$). The two floods sampled on December 29,
374 2013 and February 13, 2014 were similar, with ^{137}Cs concentrations ranging between 17.1 ± 1.1 and
375 $17 \pm 4.3 \text{ Bq kg}^{-1}$ respectively. Samples collected during the low-flow periods are characterized by low
376 ^{137}Cs activities ($6.9 \pm 0.8 \text{ Bq kg}^{-1}$ on September 10, 2013 and $13.9 \pm 12.3 \text{ Bq kg}^{-1}$ on April 30, 2014).
377 The sediment collected at the tile drain outlets ($n = 5$) were characterized by the presence of high ^{137}Cs
378 activities with an average of $23.4 \pm 4 \text{ Bq kg}^{-1}$ (ranging between 8.6 ± 0.3 and $30.6 \pm 0.5 \text{ Bq kg}^{-1}$)
379 indicative of elevated surface source contributions. As shown in Fig. 5, these high concentrations of
380 ^{137}Cs in the sediment samples mainly plot within the concentration range of surface sources. Over a
381 10-year period (2003–2013) the ^{137}Cs activity of material accumulated in the pond ranged between
382 10.9 ± 0.7 and $11.9 \pm 0.7 \text{ Bq kg}^{-1}$ with an average activity at the upper 10 cm of the core being $11.4 \pm$
383 0.5 Bq kg^{-1} . These values also plot clearly within the surface source range. Summary statistics of ^{137}Cs
384 concentrations are provided in Table 2 for all sediment samples.

385

386 3.4. Modelling results – source identification

387

388 When all sediment samples from the monitoring stations are grouped together (*C* in Eq. (3)),
389 the modelling results for both corrections indicate that sediment transported in the Louroux catchment
390 are almost entirely originated from surface sources ($99 \pm 1.2\%$ with the *SSA* correction and $94 \pm 1.5\%$
391 with the *Th* correction). Corrected ^{137}Cs activities in sediment collected at the different monitoring
392 stations clearly plots within the distribution of surface source ^{137}Cs activities (Fig. 7). The modelling
393 results averaged for the 5 monitoring stations indicate a surface contribution of 99% ($\pm 0.5\%$) with the

394 *SSA* correction. The results with the *Th* correction are comparable with a mean modelled surface
395 contribution of 98% ($\pm 1.9\%$). The mean difference between surface source contributions with the *SSA*
396 and *Th* corrections modelled for all monitoring stations was 1.2% ($\pm 1.6\%$). Table 3 lists all modelling
397 results.

398 To further examine sediment sources in this catchment, the different events sampled were
399 modelled separately. Sediment samples collected during flood events have elevated ^{137}Cs
400 concentrations (suspended sediment samples SSE2–6 in Fig. 8). These high activities indicate a major
401 contribution of surface material during the flood events. The modelled results indicate a surface source
402 contribution of 99% ($\pm 0.4\%$) with the *SSA* correction and 99% ($\pm 0.5\%$) with the *Th* correction.
403 Samples collected during a low flow event had a ^{137}Cs signature clearly lower than during the flood
404 conditions representative of a more homogeneous mixture of surface and subsurface sources (SSE1 in
405 Fig. 8). During the low flow period, the sediment distribution plotted closer to the subsurface source
406 distribution (Fig. 8). Surface sources were modelled to contribute 49% ($\pm 3.5\%$) with the *SSA*
407 correction compared to 40% ($\pm 2.1\%$) with the *Th* correction. Although there was a 9% difference
408 between the modelled results with the *SSA* and *Th* corrections for the low flow event, the mean
409 difference between the modelled surface source contributions for all events was only 2% ($\pm 3\%$).

410 The mean ^{137}Cs value of sediment at the tile drainage network outlet ($23.4 \pm 4 \text{ Bq kg}^{-1}$) was
411 higher than during the floods ($18.4 \pm 3.4 \text{ Bq kg}^{-1}$), (Figs. 6 and 7). Sediment exported from the
412 drainage network was modelled to originate predominantly from surface sources ($99 \pm 2.5\%$) with
413 both corrections (Fig. 9). This indicates that these drainage networks potentially facilitate the transfer
414 of surface soils and should be treated as a surface source in this catchment. For the sediment core,
415 results indicate that sediment is mainly derived from surface sources with a modelled contribution of
416 99% ($\pm 1.5\%$) with the *SSA* correction compared to 97% ($\pm 6.7\%$) with the *Th* correction.

417

418 **4. Discussion**

419

420 In this study the *SSA* and *Th* corrections reduced particle size enrichment impacts on ^{137}Cs
421 concentrations. The *SSA* measured for both sources were similar (subsurface mean: $340 \text{ m}^2 \text{ kg}^{-1}$,
422 surface mean: $390 \text{ m}^2 \text{ kg}^{-1}$). The significant difference between sediments and source *SSA* is
423 potentially indicative of particle size enrichment during sediment mobilization and transport processes.
424 This enrichment is highlighted by the large observed particle size difference between sources and
425 sediment. The application of both particle size corrections clearly improved the relationship between
426 sediment and their sources. When examining all modelling results, there was only a mean difference of
427 2% ($\pm 3\%$) between both corrective approaches. There was only one exception, the low flow sediment
428 sample (SSE1) where modelling approaches differed by 9%.

429 The main observed difference between the *Th* and *SSA* corrections could be because the
430 application of the *Th* correction allows a broader range of values than the *SSA* approach. Nevertheless,
431 the high values for the surface sources obtained with the *Th* correction do not seem to be outliers as
432 the drain samples have higher ^{137}Cs activities. By comparison at the sample scale, the *Th* correction is
433 more applicable than the *SSA* correction. The application of the *Th* correction to the surface source
434 samples (measured ^{137}Cs activity: $3.7 \pm 3 \text{ Bq kg}^{-1}$) changed the surface source ^{137}Cs activity to 14.3
435 Bq kg^{-1} compared to 11.4 Bq kg^{-1} with the *SSA* correction. The average ^{137}Cs activities during runoff
436 was $17 \pm 3 \text{ Bq kg}^{-1}$. The application of both corrections could be improved by collecting additional
437 sediment and source samples covering a wider range of ^{137}Cs activities.

438 The modelling results for sediment samples taken over the entire hydrological year
439 (2013/2014) and for the sediment core clearly illustrate that surface sources dominate the supply of
440 sediment in this catchment ($\mu = 97\% \pm 6.7\%$ for the sediments and $99 \pm 1.5\%$ for the sediment core).
441 These results are in agreement with the review on sediment sources in British rivers that indicated
442 surface sources dominate the supply of sediment, accounting for between 60% and 96% of the
443 sediment yields, with 85–95% being typical (Walling, 2005).

444 The sediment exported by the drainage network is characterized by higher ^{137}Cs activities than
445 the soil samples ($3.2 \pm 0.2 \text{ Bq kg}^{-1}$ for average soil samples and $23.4 \pm 4 \text{ Bq kg}^{-1}$ for drainage network
446 sediment). These high values are worthy of attention because ^{137}Cs activity concentrations are
447 expected to decrease below the plough depth in cultivated soil (He and Walling, 1997) and are nearly
448 undetectable in subsurface soil (Matisoff et al., 2002). One possibility could be that there has been
449 ^{137}Cs migration down in the soil profile in our catchment. According to previous studies (Sogon et al.,
450 1999; Walling et al., 2002; Chapman et al., 2005), macropores are a potential link between the topsoil
451 with high ^{137}Cs activities and the drainage networks. These macropores can be induced by the soil
452 properties, agricultural soil works, and vegetal activities (Oygarden et al., 1997), and they can be a
453 preferential pathway of sediment originating from the topsoil and labelled with ^{137}Cs (Jagercikova et
454 al., 2014). This direct pathway offers the best explanation for the rapid sediment transport observed by
455 Chapman et al. (2005) and potentially the high ^{137}Cs activities observed in sediment sampled in our
456 studied drainage network.

457 Another explanation is that eroded surface material is being exported through the drainage
458 network. Similarly to Walling et al. (2002), sediment samples from the studied field drains have higher
459 ^{137}Cs activities than the soil samples. This radionuclide enrichment at the drainage network outlet has
460 also been described by Sogon (1999) who demonstrated the occurrence of preferential particle size
461 selection in the upper soil and the migration of the finest particles through the tile drainage network
462 during runoff events. A combination of these factors likely explains this particle selectivity between
463 soil and drain material and additional research is required to determine the dominant transfer
464 mechanisms.

465 There are limited analyses of sediment contributions from drainage networks available in
466 France (Penven and Muxart, 1995; Sogon et al., 1999; Penven et al., 2001). Research from other
467 countries demonstrated that drainage networks provide a significant contribution to sediment export.
468 In the UK, drainage networks were clearly an important source to sediment yields accounting for
469 between 27% and 55% of sediment exported (Russell et al., 2001; Walling et al., 2002). Furthermore,
470 Foster et al. (2003) reported that drainage networks contributed more than 50% of sediment. At the
471 global scale, drainage network contributions may be significant. For instance, Macrae et al. (2007)
472 estimated >42% of annual hydrological discharge is originated from the drainage network in a
473 Canadian agricultural catchment. According to King et al. (2014), this hydrological pathway is under-
474 studied in agricultural basins. More research is required in the study area to determine whether ¹³⁷Cs
475 has migrated down through the soil profile or whether these drainage networks simply act as conduit
476 for quick transportation of surface soils to the stream network during runoff events.

477 At the global scale, previous sediment fingerprinting studies demonstrated that subsurface
478 contribution to sediment yields varied among catchments depending on several parameters such as
479 morphology and land use. Data compiled by Walling and Collins (2005) indicate that generally bank
480 erosion can contribute between 5% and 15% of sediment exported in British rivers but in some cases it
481 can exceed 40%. In the review of Haddadchi et al. (2013), subsurface erosion from channel bank
482 sources was reported to contribute typically between 15% to 30% of suspended sediment load. In
483 Australian catchments, it is not uncommon for subsurface sources to contribute more than 90% of
484 sediment load (Caitcheon et al., 2012; Olley et al., 2013; Laceby et al., 2015). Our results remain in
485 agreement with European studies, with an average riverbank contribution ranging between 11% to
486 32% for the last decade.

487 In the Louroux catchment, the majority of the sediments are exported during the flood events.
488 Modelling results indicate the dominance of the surface sources during these events whereas samples
489 collected during the lower flow periods have an increased proportion of sediments derived from
490 subsurface sources. The volume of water and sediment exported during the low flow events is often
491 insignificant compared to the volume of sediment exported during flood events, though more research
492 is required to define the relative proportion of both sources during the entire hydrological year.

493

494 5. Conclusions

495

496 This study highlights the potential of *Th* based particle size corrections. The application of this
497 correcting factor produced globally better results than the *SSA* correction. There remains, however,
498 more experimentation required to test the validity of this approach to particle size correction in various
499 environments, particularly catchments with heterogeneous geologies where *Th* may be a significant
500 discriminator between different spatial sediment sources.

501 Modelling results indicate that sediment transported during the flood events in the Louroux
502 catchment are almost entirely originated from surface sources, regardless of the correcting factor
503 employed (~ 99%). During these events, two pathways can mobilize this surface source: sheet and rill
504 erosion associated with the runoff events and the sediment exported from the drainage network which
505 was modelled to originate predominantly from surface sources ($99\% \pm 2.5\%$). During the low flow
506 period, modelling results correspond to a more homogenous mixture between surface and subsurface
507 sources with contributions of subsurface source ranging between 51% and 60%.

508 Over the last 10 years, surface sources dominated the supply of sediment with both corrections
509 in the pond ($99\% \pm 1.5\%$ to $97\% \pm 1.5\%$). Accordingly, management of deleterious sediments with
510 contaminants accumulated within the Louroux pond should focus on reducing the supply of sediment
511 from surface sources. Future research should examine the efficacy of drainage networks for
512 connecting sediments from surface sources to the stream network in more detail. Managing sediment
513 transferred through drainage networks may reduce suspended sediment loads in similar lowland
514 agricultural catchments.

515

516 Acknowledgements

517

518 The authors thank Xavier Bourrain and Jean-Noël Gautier for their advice and technical
519 support. Support from Aurelia Mathieu, Jean-Paul Bakyono and Rosalie Vandromme with soil and
520 sediment sampling is gratefully acknowledged. This work was supported by grants from the Loire-
521 Brittany Water Agency (TrackSed and Drastic projects). The authors would also like to thank the
522 anonymous reviewers for their constructive comments.

523

524

525

526

527

528 References

- 529
- 530
- 531 Ahn, Y., Nakamura, F., Mizugaki, S., 2008. Hydrology, suspended sediment dynamics and
532 nutrient loading in Lake Takkobu, a degrading lake ecosystem in Kushiro Mire,
533 northern Japan. *Environmental Monitoring and Assessment*, 145, pp. 267-281.
- 534 Ayrault, S., Le Pape, P., Evrard, O., Priadi, C.R., Quantin, C., Bonté, P., Roy-Barman, M.,
535 2014. Remanence of lead pollution in an urban river system: a multi-scale temporal
536 and spatial study in the Seine River basin, France. *Environmental Science and
537 Pollution Research*, 21(6), 4134-4148.
- 538 Bakker, M.M., Govers, G., van Doorn, A., Quetier, F., Chouvardas, D., Rounsevell, M., 2008.
539 The response of soil erosion and sediment export to land-use change in four areas of
540 Europe: The importance of landscape pattern. *Geomorphology*, 98(3-4), pp 213–226.
- 541 Berger, G., Kaechele, H., Pfeffer, H., 2006. The greening of the European common
542 agricultural policy by linking the European-wide obligation of set-aside with voluntary
543 agri-environmental measures on a regional scale. *Environmental Science & Policy*
544 9(6), pp 509-524.
- 545 Boardman, J., Poesen, J., 2006. Soil erosion in Europe: major processes, causes and
546 consequences. In: J.Boardman and J. Poesen (Editors), *Soil erosion in Europe*. Wiley,
547 Chichester. pp. 479-489.
- 548 Brown, A., 1985. The potential use of pollen in the identification of suspended sediment
549 sources. *Earth Surface Processes and Landforms*, 10, 27 - 32.
- 550 Caitcheon, G.G., Olley, J.M., Pantus, F., Hancock, G., Leslie, C., 2012. The dominant erosion
551 processes supplying fine sediment to three major rivers in tropical Australia, the Daly
552 (NT), Mitchell (Qld) and Flinders (Qld) Rivers. *Geomorphology*, 151-152(No), pp
553 188-195.
- 554 Carter, J., Owens, P.N., Walling, D.E., Leeks, G.J.L., 2003. Fingerprinting suspended
555 sediment sources in a large urban river system. *Science of The Total Environment*,
556 314-316(0), pp. 513-534.
- 557 Cerdan, O., Bissonnais, Y.L., Souchère, V., Martin, P., Lecomte, V., 2002. Sediment
558 concentration in interrill flow: interactions between soil surface conditions, vegetation
559 and rainfall. *Earth Surface Processes and Landforms*, 27(2), pp. 193-205.
- 560 Cerdan, O., Govers, G., Le Bissonnais, Y., Van Oost, K., Poesen, J., Saby, N., Gobin, A.,
561 Vacca, A., Quinton, J., Auerswald, K., Klik, A., Kwaad, F.J.P.M., Raclot, D., Ionita,
562 I., Rejman, J., Rousseva, S., Muxart, T., Roxo, M.J., Dostal, T., 2010. Rates and
563 spatial variations of soil erosion in Europe: A study based on erosion plot data.
564 *Geomorphology*, 122(1-2), 167-177.
- 565 Chapman, A.S., Foster, I.D.L., Lees, J.A., Hodgkinson, R.A., 2005. Sediment delivery from
566 agricultural land to rivers via subsurface drainage. *Hydrological Processes*, 19(15), pp
567 2875-2897.
- 568 Chartin, C., Evrard, O., Salvador-Blanes, S., Hinschberger, F., Van Oost, K., Lefèvre, I.,
569 Daroussin, J., Macaire, J.-J., 2011. Quantifying and modelling the impact of land
570 consolidation and field borders on soil redistribution in agricultural landscapes (1954-
571 2009). *CATENA*, 110(0), 184-195.
- 572 Collins, A.L, Walling, D.E., Leeks, G.J.L., 1996. Composite fingerprinting of the spatial
573 source of fluvial suspended sediment : a case study of the Exe and Severn river basins,
574 United Kingdom. . *Géomorphologie : relief, processus, environnement*, 2(2), pp. 41-
575 53.

576 Collins, A.L., Walling, D.E., Sickingabula, H.M., Leeks, G.J.L., 2001. Suspended sediment
577 source fingerprinting in a small tropical catchment and some management
578 implications. *Applied Geography*, 21(4), pp. 387-412.

579 Collins, A.L., Walling, D.E., 2002. Selecting fingerprint properties for discriminating
580 potential suspended sediment sources in river basins. *Journal of Hydrology*, 261, 218 -
581 244.

582 Collins, A.L., Zhang, Y., Walling, D.E., Grenfell, S.E., Smith, P., 2010. Tracing sediment loss
583 from eroding farm tracks using a geochemical fingerprinting procedure combining
584 local and genetic algorithm optimisation. *Science of The Total Environment*, 408(22),
585 pp 5461–5471.

586 Dearing, J.A., Jones, R.T., 2003. Coupling temporal and spatial dimensions of global
587 sediment flux through lake and marine sediment records. *Global and Planetary
588 Change*, 39(1-2), pp. 147-168.

589 Desmet, M., Mourier, B., Mahler, B.J., Van Metre, P.C., Roux, G., Persat, H., Lefèvre, I.,
590 Peretti, A., Chapron, E., Simonneau, A., Miège, C., Babut, M., 2012. Spatial and
591 temporal trends in PCBs in sediment along the lower Rhône River, France. *Science of
592 The Total Environment*, 433(0), 189-197.

593 European Environment Agency, 2002. EEA-ETC/TE. 2002. CORINE land cover update.
594 I&CLC2000 project. Technical guidelines, <http://terrestrial.eionet.eu.int>.

595 Evrard, O., Vandaele, K., van Wesemael, B., Bielders, C.L., 2008. A grassed waterway and
596 earthen dams to control muddy floods from a cultivated catchment of the Belgian loess
597 belt. *Geomorphology*, 100(34), 419-428.

598 Evrard, O., Nord, G., Cerdan, O., Souchère, V., Le Bissonnais, Y., Bonté, P., 2010. Modelling
599 the impact of land use change and rainfall seasonality on sediment export from an
600 agricultural catchment of the northwestern European loess belt. *Agriculture,
601 Ecosystems & Environment*, 138(1-2), pp. 83-94.

602 Evrard, O., Navratil, O., Ayrault, S., Ahmadi, M., Némery, J., Legout, C., Lefèvre, I., Poirel,
603 A., Bonté, P., Esteves, M., 2011. Combining suspended sediment monitoring and
604 fingerprinting to determine the spatial origin of fine sediment in a mountainous river
605 catchment. *Earth Surface Processes and Landforms*, 36, 1072-1089.

606 Evrard, O., Van Beek, P., Gateuille, D., Pont, V., Lefèvre, I., Lansard, B., Bonté, P., 2012.
607 Evidence of the radioactive fallout in France due to the Fukushima nuclear accident.
608 *Journal of environmental radioactivity*, 114, 54-60.

609 Evrard, O., Chartin, C., Onda, Y., Lepage, H., Cerdan, O., Lefèvre, I., Ayrault, S., 2014.
610 Renewed soil erosion and remobilisation of radioactive sediment in Fukushima coastal
611 rivers after the 2013 typhoons. *Sci. Rep.*, 4.

612 Foster, I.D.L., Walling, D.E., 1994. Using reservoir deposits to reconstruct changing sediment
613 yields and sources in the catchment of the Old Mill Reservoir, South Devon, UK, Over
614 the past 50 years. *hydrological Sciences*(39), 347 - 368.

615 Foster, I.D.L., Chapman, A.S., Hodgkinson, R.M., Jones, A.R., Lees, J.A., Turner, S.E., Scott,
616 M., 2003. Changing suspended sediment and particulate phosphorus loads and
617 pathways in underdrained lowland agricultural catchments; Herefordshire and
618 Worcestershire, U.K. *Hydrobiologia*, 494(1), 119-126.

619 Foucher, A., Salvador-Blanes, S., Desmet, M., Simonneau, A., Chapron, E., Evrard, O.,
620 Courp, T., Cerdan, O., Lefèvre, I., Adriaensen, H., Lecompte, F., 2015. Increased
621 erosion and sediment yield in a lowland catchment following the intensification of
622 agriculture (Louroux catchment, Loire Valley, France, 1950-2010). *Anthropocene*.

623 Froger, D., Moulin, J., Servant, J., 1994. Les terres de Gatines, Boischaud-Nord, Pays-Fort,
624 Touraine-Berry. *Typologie des sols. Chambres d'agriculture du Cher, de l'Indre, de
625 l'Indre et Loire et du Loire et Cher.*

- 626 Haddadchi, A., Ryder, D.S., Evrard, O., Olley, J., 2013. Sediment fingerprinting in fluvial
627 systems: review of tracers, sediment sources and mixing models. *International Journal*
628 *of Sediment Research*, 28(4), 560-578.
- 629 He, Q., Owens, P.N., 1995. Determination of suspended sediment provenance using caesium-
630 137, unsupported lead-210 and radium-226: a numerical mixing model approach.
631 *Sediment and Water Quality in River Catchments*, pp. 207–227.
- 632 He, Q., Walling, D.E., 1996. Interpreting particle size effects in the adsorption of 137Cs and
633 unsupported 210Pb by mineral soils and sediments. *Journal of Environmental*
634 *Radioactivity*, 30, pp. 117–137.
- 635 He, Q., Walling, D.E., 1997. The distribution of fallout 137Cs and 210Pb in undisturbed and
636 cultivated soils. *Applied Radiation and Isotopes*, 48(5), pp 677-690.
- 637 Horowitz, A.J., Elrick, K.A., 1987. The relation of stream sediment surface area, grain size
638 and composition to trace element chemistry. *Applied Geochemistry*, 2(4), pp. 437-451.
- 639 Horowitz, A.J., 2008. Determining annual suspended sediment and sediment-associated trace
640 element and nutrient fluxes. *Science of The Total Environment*, 400, 315.
- 641 Jagercikova, M., Evrard, O., Balesdent, J., Lefèvre, I., Cornu, S., 2014. Modeling the
642 migration of fallout radionuclides to quantify the contemporary transfer of fine
643 particles in Luvisol profiles under different land uses and farming practices. *Soil and*
644 *Tillage Research*, 140(0), pp. 82-97.
- 645 Jones, A., Panagos, P., Barcelo, S., Bouraoui, F., Bosco, C., Dewitte, O., Gardi, C., Erhard,
646 M., Hervás, J., Hiederer, R., Jeffery, S., Lükewille, A., Marmo, L., Montanarella, L.,
647 Olazábal, C., Petersen, J., Penizek, V., Strassburger, T., Tóth, G., Van Den Eeckhaut,
648 M., Van Liedekerke, M., Verheijen, F., Viestova, E., Yigini, Y., 2012. The state of soil
649 in Europe (SOER). JRC reference reports. Report 25186 EN.
650 http://ec.europa.eu/dgs/jrc/downloads/jrc_reference_report_2012_02_soil.pdf, 80 pp.
- 651 King, K.W., Fausey, N.R., Williams, M.R., 2014. Effect of subsurface drainage on
652 streamflow in an agricultural headwater watershed. *Journal of Hydrology*, 519, Part A,
653 pp 438-445.
- 654 Koiter, A.J., Owens, P.N., Petticrew, E.L., Lobb, D.A., 2013. The behavioural characteristics
655 of sediment properties and their implications for sediment fingerprinting as an
656 approach for identifying sediment sources in river basins. *Earth-Science Reviews*, 125,
657 24-42.
- 658 Kronvang, B., Laubel, A., Grant, R., 1997. Suspended sediment and particulate phosphorus
659 transport and delivery pathways in an arable catchment, Gelbaek stream, Denmark.
660 *Hydrological Processes*, 11(6), pp. 627-642.
- 661 Kronvang, B., Kronvang, B., Laubel, A., Larsen, S.E., Friberg, N., 2003. Pesticides and heavy
662 metals in Danish streambed sediment, *The Interactions between Sediments and Water.*
663 *Developments in Hydrobiology.* Springer Netherlands, pp. 93-101.
- 664 Lacey, J.P., Olley, J., 2015. An examination of geochemical modelling approaches to tracing
665 sediment sources incorporating distribution mixing and elemental correlations.
666 *Hydrological Processes*, n/a.
- 667 Lacey, J. P., Olley, J., Pietsch, T. J., Sheldon, F. and Bunn, S. E., 2015. Identifying subsoil
668 sediment sources with carbon and nitrogen stable isotope ratios. *Hydrolog.*
669 *Process.*, 29: 1956–1971
- 670 Macrae, M.L., English, M.C., Schiff, S.L., Stone, M., 2007. Intra-annual variability in the
671 contribution of tile drains to basin discharge and phosphorus export in a first-order
672 agricultural catchment. *Agricultural Water Management*, 92(3), pp 171-182.
- 673 Martinez-Carreras, N., Udelhoven, T., Krein, A., Gallart, F., Iffly, J.F., Ziebel, J., Hoffmann,
674 L., Pfister, L., Walling, D.E., 2010. The use of sediment colour measured by diffuse

675 reflectance spectrometry to determine sediment sources: Application to the Attert
676 River catchment (Luxembourg). *Journal of Hydrology*, 382, p 49-63.

677 Matisoff, G., Bonniwell, E.C., Whiting, P.J., 2002. Soil erosion and sediment sources in an
678 Ohio watershed using Beryllium-7, Cesium-137, and Lead-210. *Journal of*
679 *Environmental Quality*(31), 54-61.

680 Motha, J.A., Wallbrink, P.J., Hairsine, P.B., Grayson, R.B., 2002. Tracer properties of eroded
681 sediment and source material. *Hydrological Processes*, 16(10), pp 1983-2000.

682 Nakamura, F., Kameyama, S., Mizugaki, S., 2004. Rapid shrinkage of Kushiro Mire, the
683 largest mire in Japan, due to increased sedimentation associated with land-use
684 development in the catchment. *CATENA*, 55(2), 213.

685 Navratil, O., Evrard, O., Esteves, M., Legout, C., Ayrault, S., Némery, J., Mate-Marin, A.,
686 Ahmadi, M., Lefèvre, I., Poirel, A., Bonté, P., 2012. Temporal variability of
687 suspended sediment sources in an alpine catchment combining river/rainfall
688 monitoring and sediment fingerprinting. *Earth Surface Processes and Landforms*.

689 Olley, J., Caitcheon, G., 2000. Major element chemistry of sediments from the Darling-
690 Barwon river and its tributaries: implications for sediment and phosphorus sources.
691 *Hydrological Processes*, 14(7), 1159-1175.

692 Olley, J., Burton, J., Smolders, K., Pantus, F., Pietsch, T., 2013. The application of fallout
693 radionuclides to determine the dominant erosion process in water supply catchments
694 885-895.

695 Owens, P.N., Walling, D.E., 2002. The phosphorus content of fluvial sediment in rural and
696 industrialized river basins. *Water Research*, 36, pp. 685-701.

697 Owens, P.N., Batalla, R.J., Collins, A.J., Gomez, B., Hicks, D.M., Horowitz, A.J., Kondolf,
698 G.M., Marden, M., Page, M.J., Peacock, D.H., Petticrew, E.L., Salomons, W.,
699 Trustrum, N.A., 2005. Fine-grained sediment in river systems: environmental
700 significance and management issues. *River Research and applications*, 21(7), 693-717.

701 Oygarden, L., Kvaerner, J., Jenssen, P.D., 1997. Soil erosion via preferential flow to drainage
702 systems in clay soils. *Geoderma*, 76, pp 65-86.

703 Penven, M.-J., Muxart, T., 1995. Le drainage agricole : un rôle fondamental dans les
704 transferts d'eau et de matière. L'exemple du plateau briard. *Annales de Géographie*,
705 104(n° 581 - 582), 88 - 104 p.

706 Penven, M.-J., Muxart, T., Cosandey, C., Andreu, A., 2001. Contribution du drainage agricole
707 enterré à l'érosion des sols en région tempérée (BRIE). pp 128 - 144.

708 Pulley, S., Foster, I., Antunes, P., 2015. The uncertainties associated with sediment
709 fingerprinting suspended and recently deposited fluvial sediment in the Nene river
710 basin. *Geomorphology*, 228(0), pp. 303-319.

711 Rasplus, L., Macaire, J.J., Alcaydé, G., 1982. Carte géologique de Bléré au 1:5000, Editions
712 BRGM.

713 Russell, M.A., Walling, D.E., Hodgkinson, R.A., 2001. Suspended sediment sources in two
714 small lowland agricultural catchments in the UK. *Journal of Hydrology*, 252, p 1-24.

715 Sakaguchi, A., Yamamoto, M., Sasaki, K., Kashiwaya, K., 2006. Uranium and Thorium
716 Isotope Distribution in an Offshore Bottom Sediment Core of the Selenga Delta, Lake
717 Baikal, Siberia. *Journal of Paleolimnology*, 35(4), 807-818.

718 Sharma, A., Tiwari, K., Bhadoria, P.B.S., 2011. Effect of land use land cover change on soil
719 erosion potential in an agricultural watershed. *Environmental Monitoring and*
720 *Assessment*, 173(1-4), 789-801.

721 Smith, H.G., Blake, W.H., 2014. Sediment fingerprinting in agricultural catchments: A
722 critical re-examination of source discrimination and data corrections. *Geomorphology*,
723 204(0), 177.

- 724 Sogon, S., 1999. Erosion des sols cultivés et transport des matières en suspension dans un
 725 bassin versant de Brie. Application des traceurs radioactifs naturels et magnétiques.
 726 Université Paris1 - Panthéon-Sorbonne. Thèse, 305 p.
- 727 Sogon, S., Penven, M.J., Bonte, P., Muxart, T., 1999. Estimation of sediment yield and soil
 728 loss using suspended sediment load and ^{137}Cs measurements on agricultural land,
 729 Brie Plateau, France. *Hydrobiologia*, 410(0), 251-261.
- 730 Wallbrink, P.J., Murray, A.S., 1996. Distribution and Variability of ^7Be in Soils Under
 731 Different Surface Cover Conditions and its Potential for Describing Soil
 732 Redistribution Processes. *Water Resources Research*, 32(2), pp 467-476.
- 733 Wallbrink, P.J., Olley, J.M., Murray, A.S., Olive, L.J., 1996. The contribution of subsoil to
 734 sediment yield in the Murrumbidgee River basin, New South Wales, Australia.
 735 Erosion and sediment yield: global and regional perspectives. (Proceedings Exeter
 736 symposium, 1996). IAHS Publication, 236, pp. 347–355.
- 737 Wallbrink, P.J., 2004. Quantifying the erosion processes and land-uses which dominate fine
 738 sediment supply to Moreton Bay, Southeast Queensland, Australia. *Journal of*
 739 *Environmental Radioactivity*, 76.
- 740 Walling, D.E., Woodward, J.C., Nicholas, A.P., 1993. A multi-parameter approach to
 741 fingerprinting suspended-sediment sources, IAHS publication.
- 742 Walling, D.E., Russell, M.A., Hodgkinson, R.A., Zhang, Y., 2002. Establishing sediment
 743 budgets for two small lowland agricultural catchments in the UK. *CATENA*, 47(4),
 744 323-353.
- 745 Walling, D.E., Owens, P.N., Foster, I.D.L., Lees, J.A., 2003. Changes in the fine sediment
 746 dynamics of the Ouse and Tweed basins in the UK over the last 100–150 years.
 747 *Hydrological Processes*, 17(16), 3245.
- 748 Walling, D.E., 2005. Tracing suspended sediment sources in catchments and river systems.
 749 *Science of The Total Environment*, 344, pp 159-184.
- 750 Walling, D.E., Collins, A.L., 2005. *Sediment Budgets*, IAHS Press, Wallingford 123–133.
- 751 Wood, P.J., Armitage, P.D., 1997. Biological Effects of Fine Sediment in the Lotic
 752 Environment. *Environmental Management*, 21(2), 203-217.

753
 754
 755
 756

757 Figure captions:

758
 759

760 Fig. 1. Catchment and sampling location map with, A) the location of the study site in the Loire River
 761 basin, and B) the Louroux pond catchment with source sample locations and river monitoring sites
 762 (S1: Beaulieu River, S2: Grand Bray River, S3: Masnier River, S4: Picarderie River, S5: Conteraye
 763 River and D1–3: drain stations, H: Hillslope sediment samples collected during runoff events).

764

765 Fig. 2. ^{137}Cs activities in multiple particle size fractions, (bulk soil and fractions ranging 63–50, 50–20,
 766 or <20 μm) and suspended sediment (SS).

767

768 Fig. 3. Relationship between $^{210}\text{Pb}_{\text{ex}}$ and ^{137}Cs for surface and subsurface sources along with in-stream
 769 sediments.

770

771 Fig. 4. Relationship between measured and corrected ^{137}Cs activities for the surface and subsurface
772 samples using the *SSA* (A) and *Th* (B) correcting factors. Error bars represent analytical uncertainties
773 on radionuclide activities (1 sigma).

774

775 Fig. 5. Relationship between $^{210}\text{Pb}_{\text{ex}}$ and ^{137}Cs for surface and subsurface sources along with in-stream
776 sediments after the *SSA* (A) and *Th* (B) particle size corrections.

777

778 Fig. 6. Probability plots characterizing surface and subsurface sample distributions with the *SSA* (A)
779 and *Th* (B) particle size corrections. The probabilities were generated for each source with 2500 Latin
780 hypercube samples from each source distribution.

781

782 Fig. 7. Probability plots for ^{137}Cs activity concentrations including sediment samples (black squares)
783 collected from the monitoring sites. In each case, probabilities were generated with 2500 Latin
784 hypercube samples from the source and sediment distributions as well as the mixture distribution.
785 Error bars represent analytical uncertainties of sediment samples equivalent to one standard error of
786 the mean. The solid line is the subsurface source distribution, the dashed line is the surface source
787 distribution and the dotted line is the distribution of sediment from each monitoring station.

788

789 Fig. 8. Probability plots for ^{137}Cs activity concentrations including sediment samples (black circles)
790 collected during the six sampling survey (SSE1: 09 Sept 2013; SSE2: 30 Dec 2013; SSE3: 29 Jan
791 2014; SSE4: 13 Feb 2014; SSE5: 4 Apr 2014; SSE6: 30 Apr 2014). In each case, probabilities were
792 generated with 2500 Latin hypercube samples from the source and sediment distributions as well as
793 the mixture distribution. Error bars represent analytical uncertainties of sediment samples equivalent
794 to one standard error of the mean. The solid line is the subsurface source distribution, the dashed line
795 is the surface source distribution and the dotted line is the distribution of sediment from each event
796 sampled.

797

798 Fig. 9. Probability plots for ^{137}Cs activity concentrations including the core and tile drainage network
799 samples (black circles). In each case, probabilities were generated with 2500 Latin hypercube samples
800 from the source and sediment distributions as well as the mixture distribution. Error bars represent
801 analytical uncertainties of sediment samples equivalent to one standard error of the mean. The solid
802 line is the subsurface source distribution, the dashed line is the surface source distribution and the
803 dotted line is the distribution of sediment from core and tile drainage network.

804

805 Table captions:

806

807 Table 1. Summary of ^{137}Cs activities (Bq kg^{-1}) of the potential sources with the different correction
808 techniques (w/o corr: without correction, *SSA*: surface specific correction, *Th*: Thorium correction).

809

810 Table 2. Summary of mean ^{137}Cs activities and the standard deviation (σ) (Bq kg^{-1}) for the in-stream
811 and drain samples at each monitoring station during flood events.

812

813 Table 3. Details of modeling results for surface and subsurface contributions.

814

815

Table 1

Statistic	Subsoil			Surface		
	<i>w/o corr.</i>	<i>SSA</i>	<i>Th</i>	<i>w/o corr.</i>	<i>SSA</i>	<i>Th</i>
Mean	1.3	1.7	1.8	3.2	10.0	11.2
Standard deviation	1.0	1.9	2.2	1.4	4.2	8.3
Mediane	1.0	1.3	0.9	2.9	9.3	9.3
Minimum	0.0	-0.7	0.0	1.0	3.7	0.8
Maximum	3.1	5.1	6.5	7.9	23.8	35.5

Table 2

	Date	^{137}Cs	σ
Station 1	09/09/2013	8.6	0.7
	30/12/2013	21.3	4.2
	29/01/2014	20.3	1.6
	13/02/2014	16.9	0.8
	04/04/2014	10.3	3.2
Station 2	09/09/2013	6.0	0.6
	30/12/2013	24.6	4.4
	29/01/2014	18.3	2.1
	13/02/2014	17.8	1.0
Station 3	30/12/2013	6.3	2.4
	29/01/2014	25.1	3.1
	13/02/2014	14.3	0.9
	04/04/2014	30.2	13.2
	30/04/2014	0.0	17.3
Station 4	09/09/2013	7.1	1.1
	30/12/2013	11.5	5.1
	29/01/2014	23.1	2.4
	13/02/2014	15.4	0.8
	30/04/2014	31.3	8.6
Station 5	09/09/2013	6.1	1.0
	30/12/2013	25.5	5.3
	29/01/2014	36.7	4.7
	13/02/2014	21.3	1.8
	04/04/2014	18.8	5.4
	30/04/2014	24.4	7.7
D1	30/12/2013	13.4	2.3
	29/01/2014	23.5	4.1
D2	16/01/2013	8.6	0.3
D3	30/12/2013	30.6	7.5
	29/01/2014	26.1	2.3

Table 3

Type	Surface contribution (%) and standard error (%)			
	<i>SSA</i>		<i>Th</i>	
Average sample	99	± 2	94	± 1.5
Sediment Core	99	± 1.5	97	± 6.7
Drain sediment	99	± 2	99	± 2.5
Station 1	99	± 1	96	± 2
Station 2	98	± 1.6	95	± 1.5
Station 3	99	± 1	99	± 1
Station 4	99	± 1.2	99	± 1
Station 5	99	± 1.1	99	± 1.2
SSE1- 09 sep 13	49	± 3.5	40	± 2
SSE2- 30 dec 13	98	± 1	99	± 1.4
SSE3- 29 jan 14	99	± 1	99	± 1
SSE4- 13 feb 14	99	± 2	98	± 1.5
SSE5- 04 apr 14	99	± 1	99	± 2
SSE6- 30 apr 14	98	± 1.5	99	± 3

Fig. 1

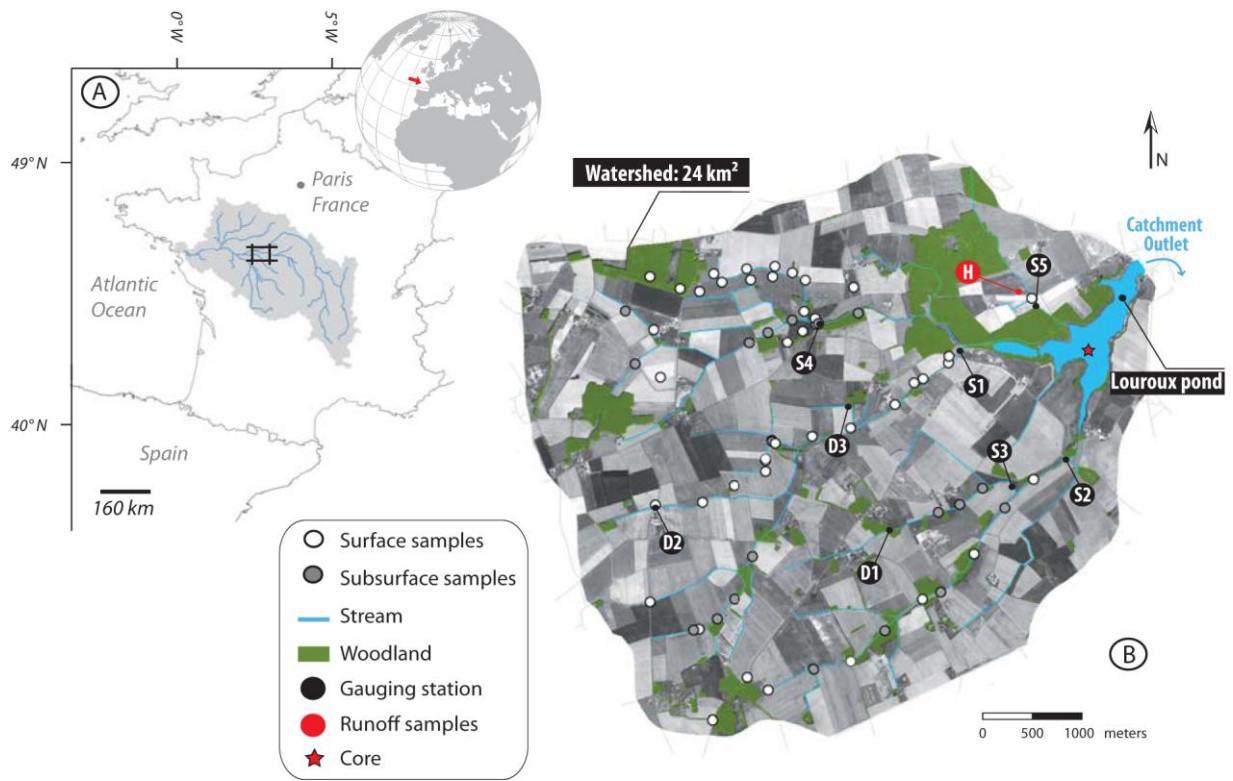


Fig. 2

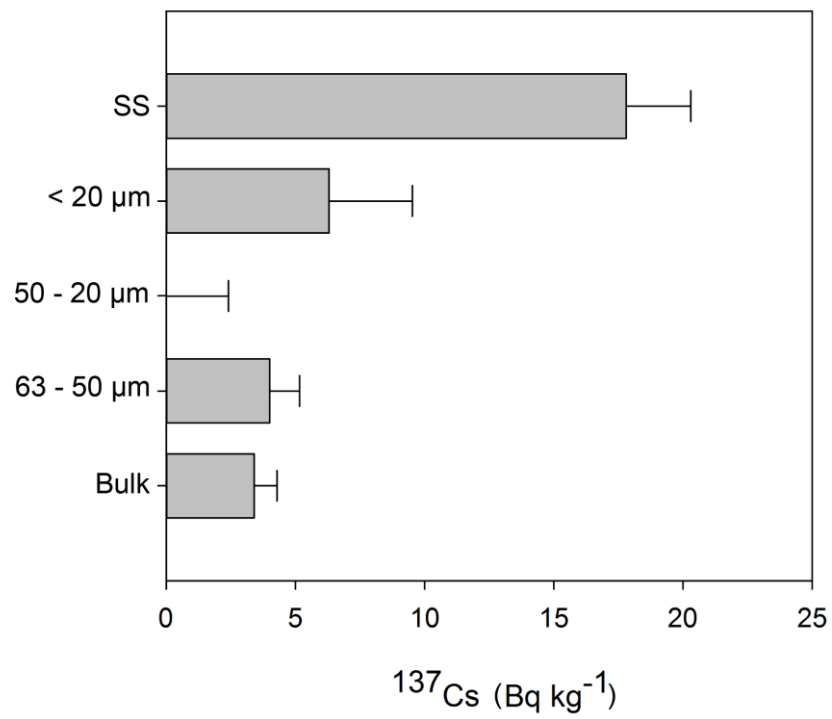


Fig. 3

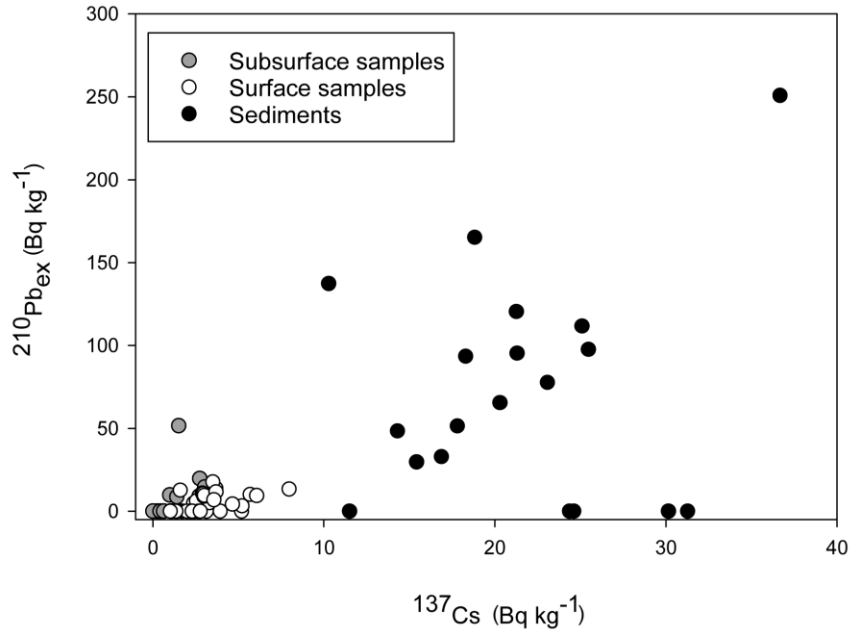


Fig. 4

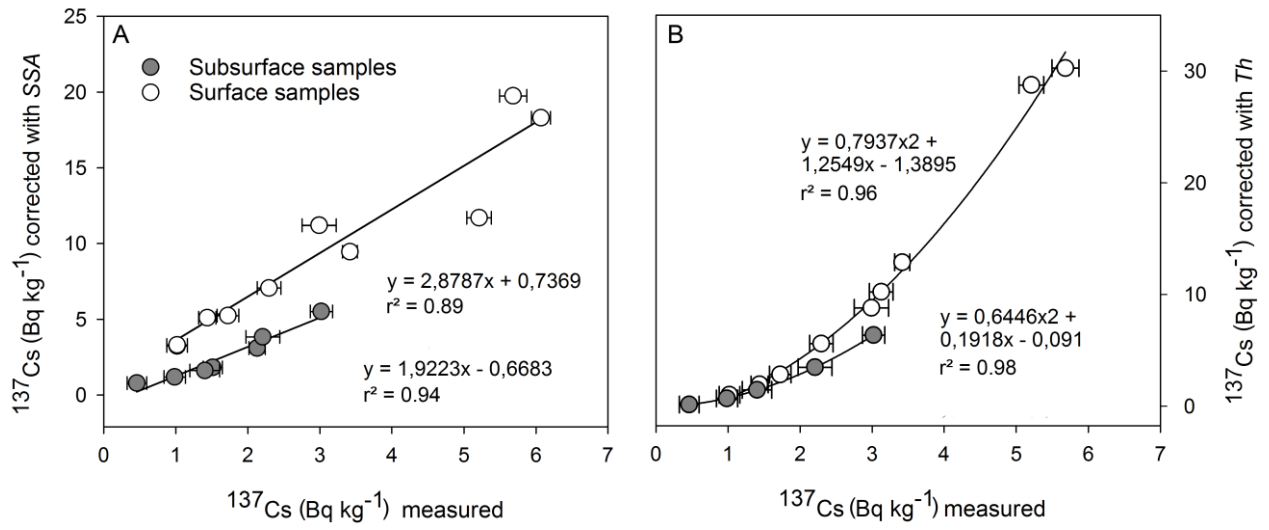


Fig. 5

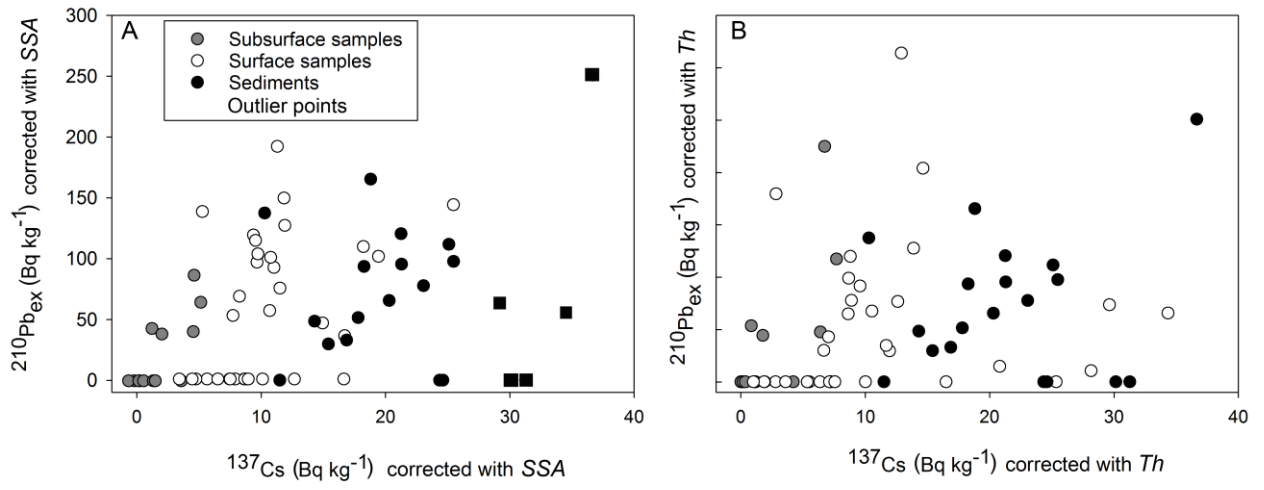


Fig. 6

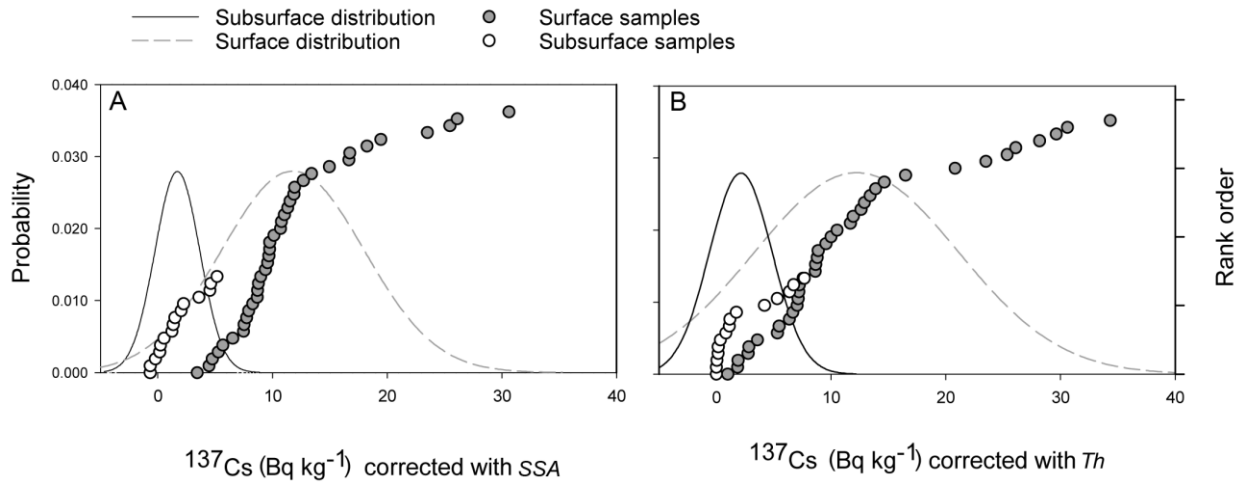


Fig. 7

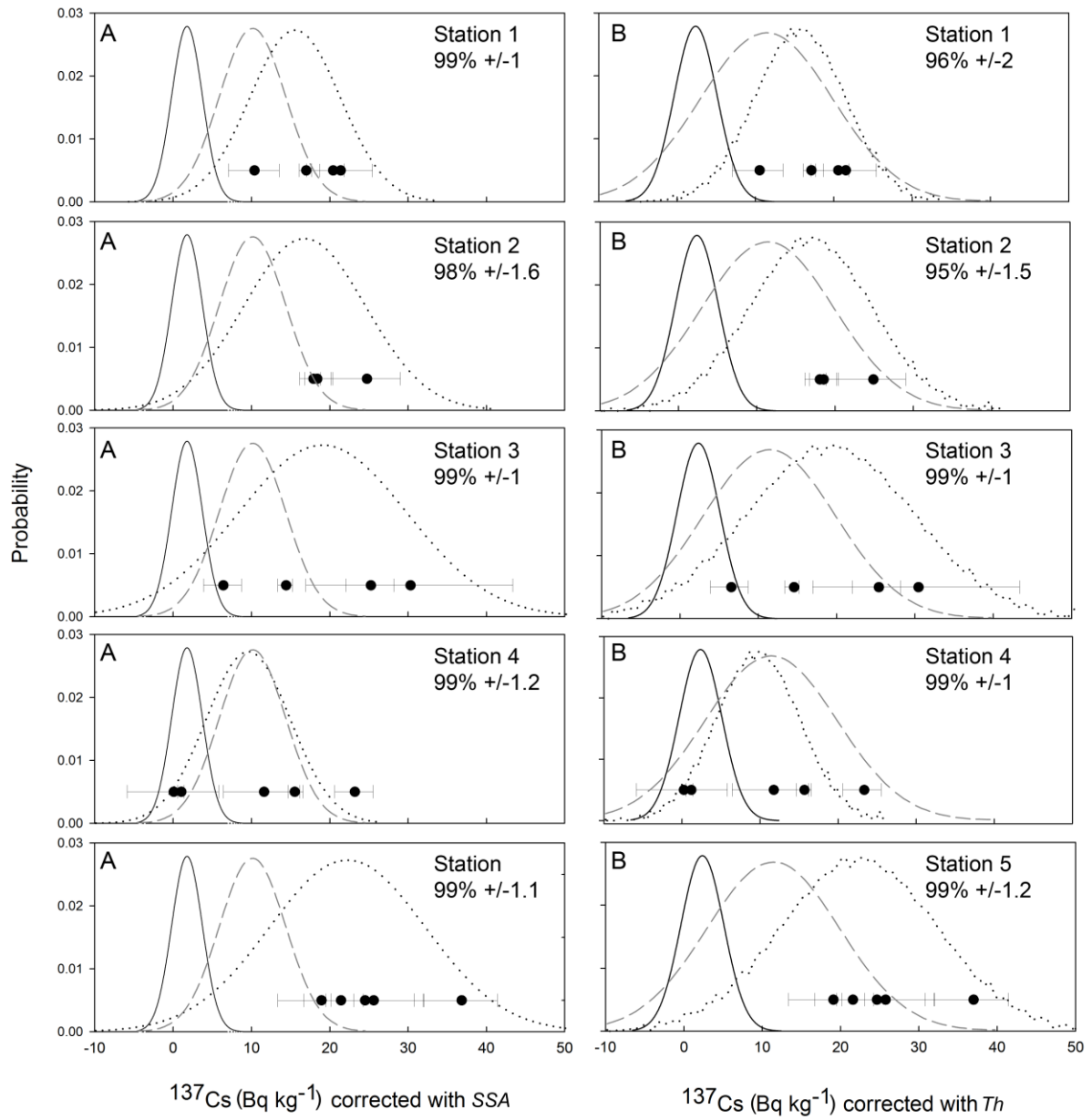


Fig. 8

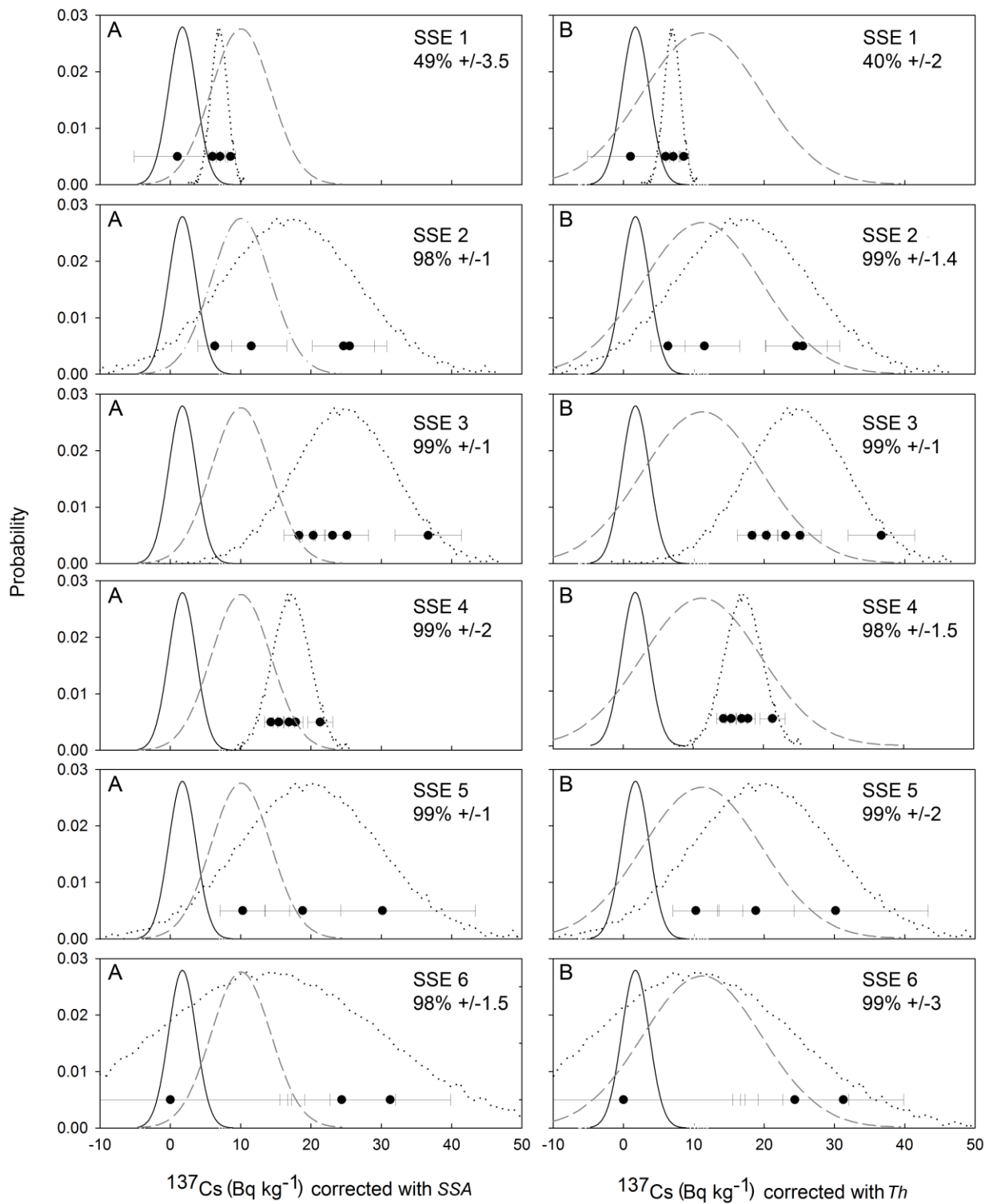


Fig. 9

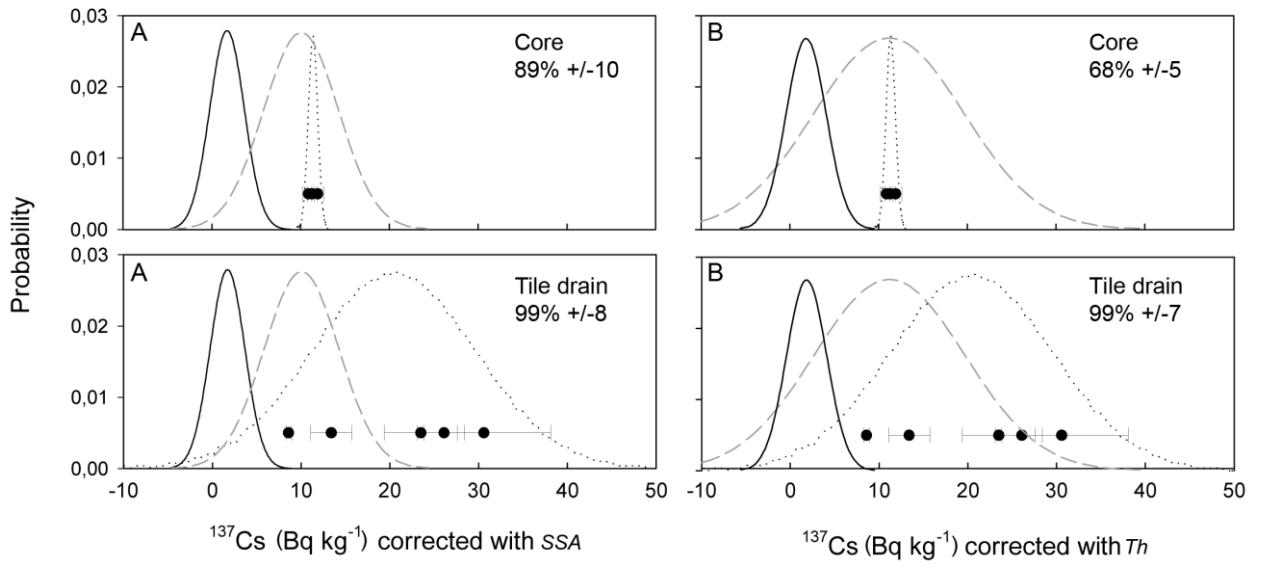


Fig. 1

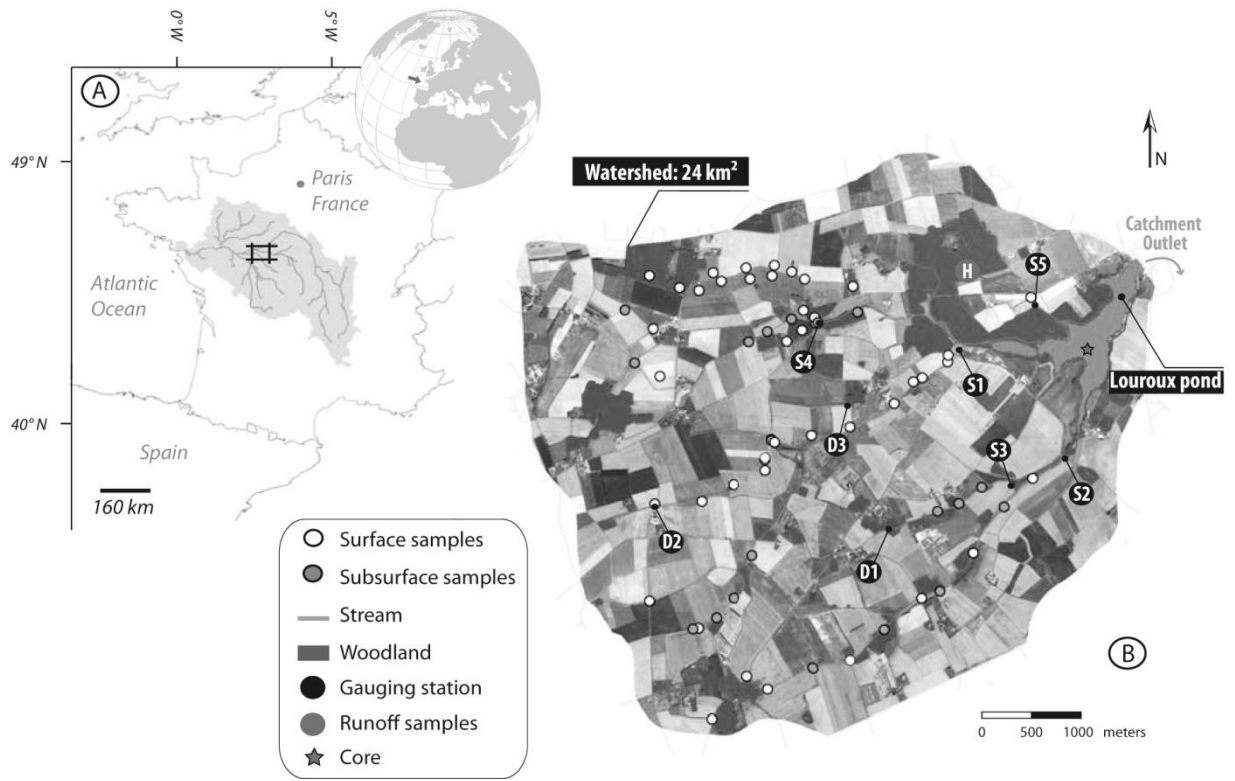


Fig. 2

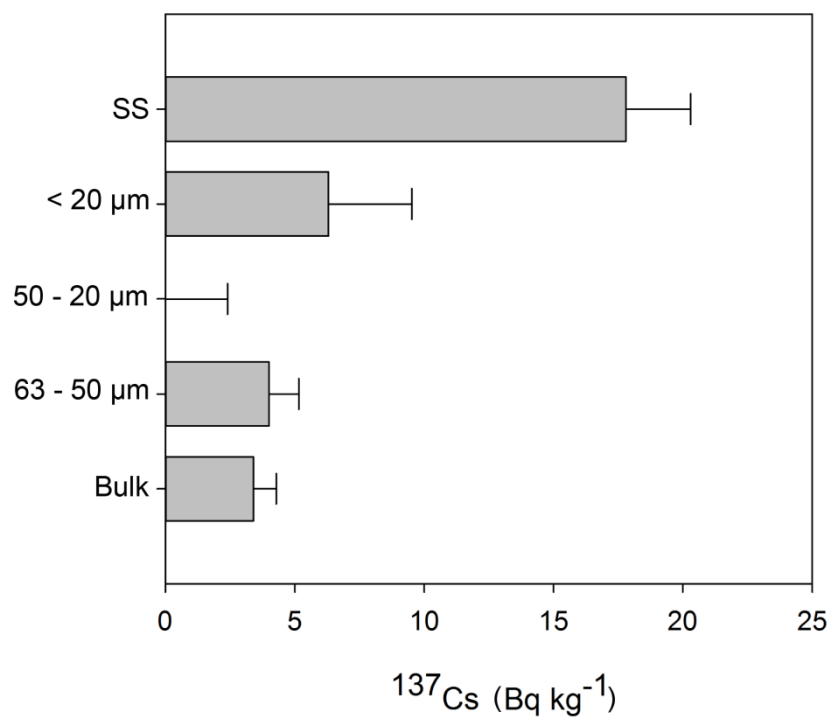


Fig. 3

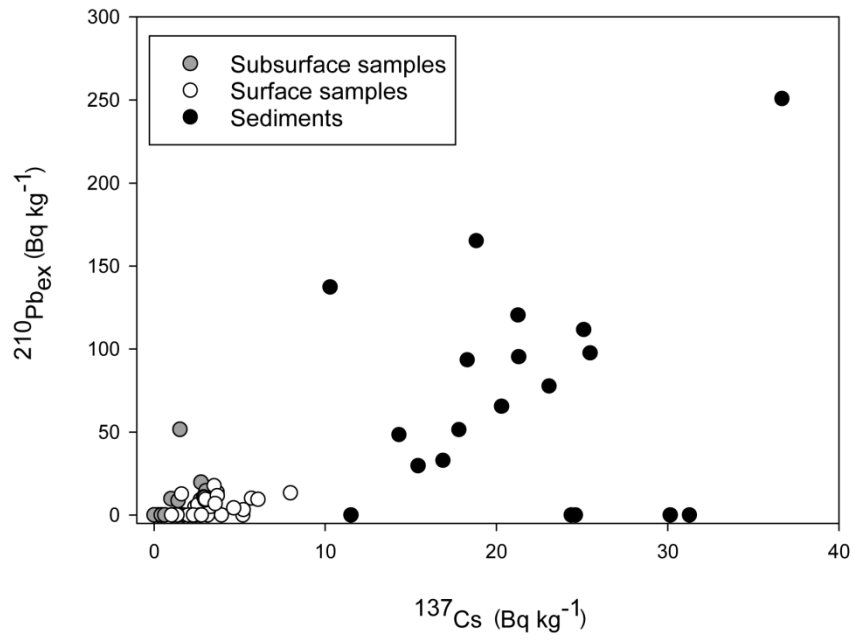


Fig. 4

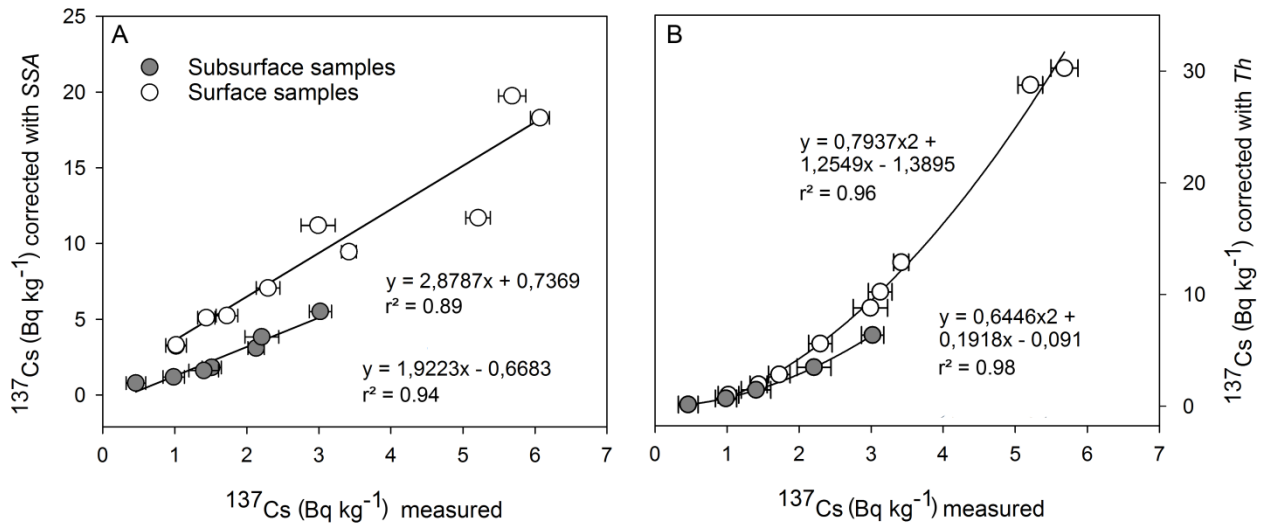


Fig. 5

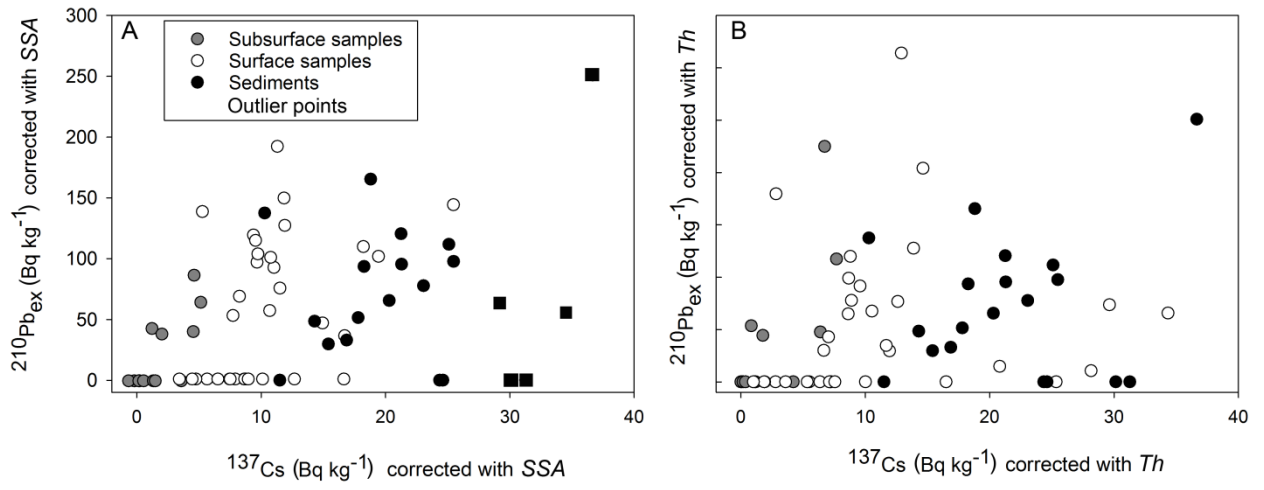


Fig. 6

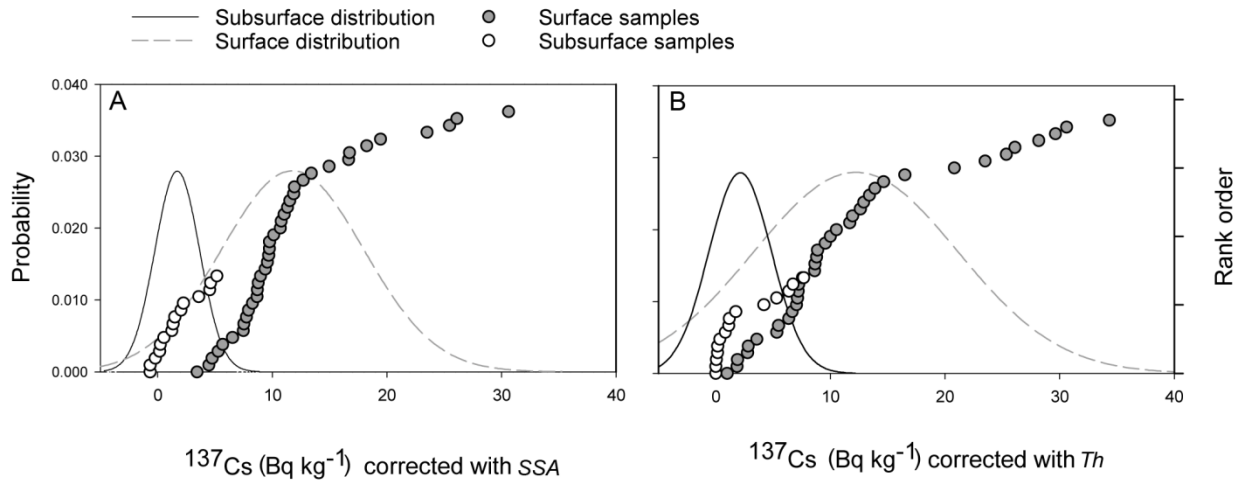


Fig. 7

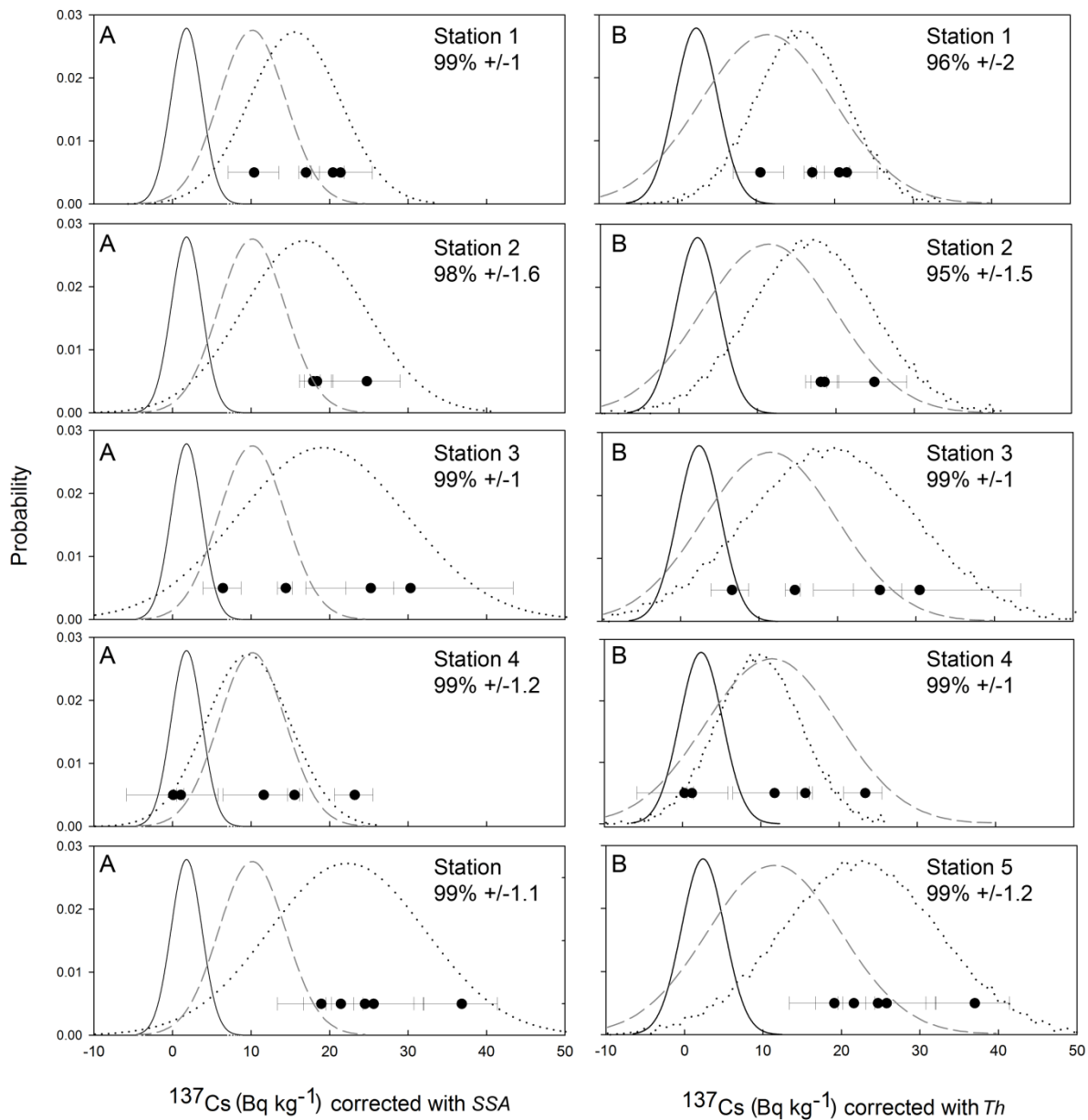


Fig. 8

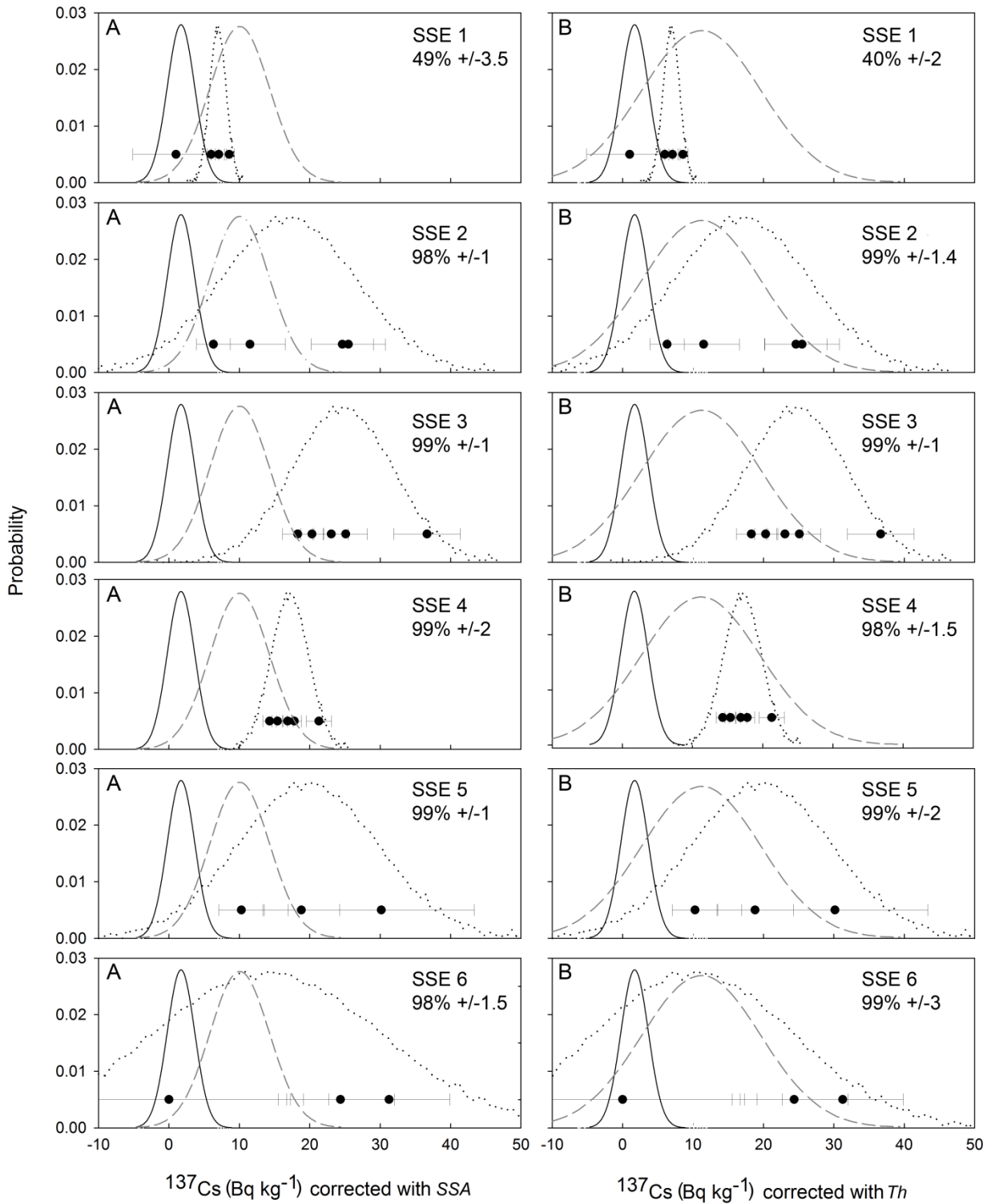


Fig. 9

